Optimisation and Application of Nanoelectroporation for Clonal β-Cell Transfection

Ekstrand, Frida

2025

Document Version:
Publisher's PDF, also known as Version of record

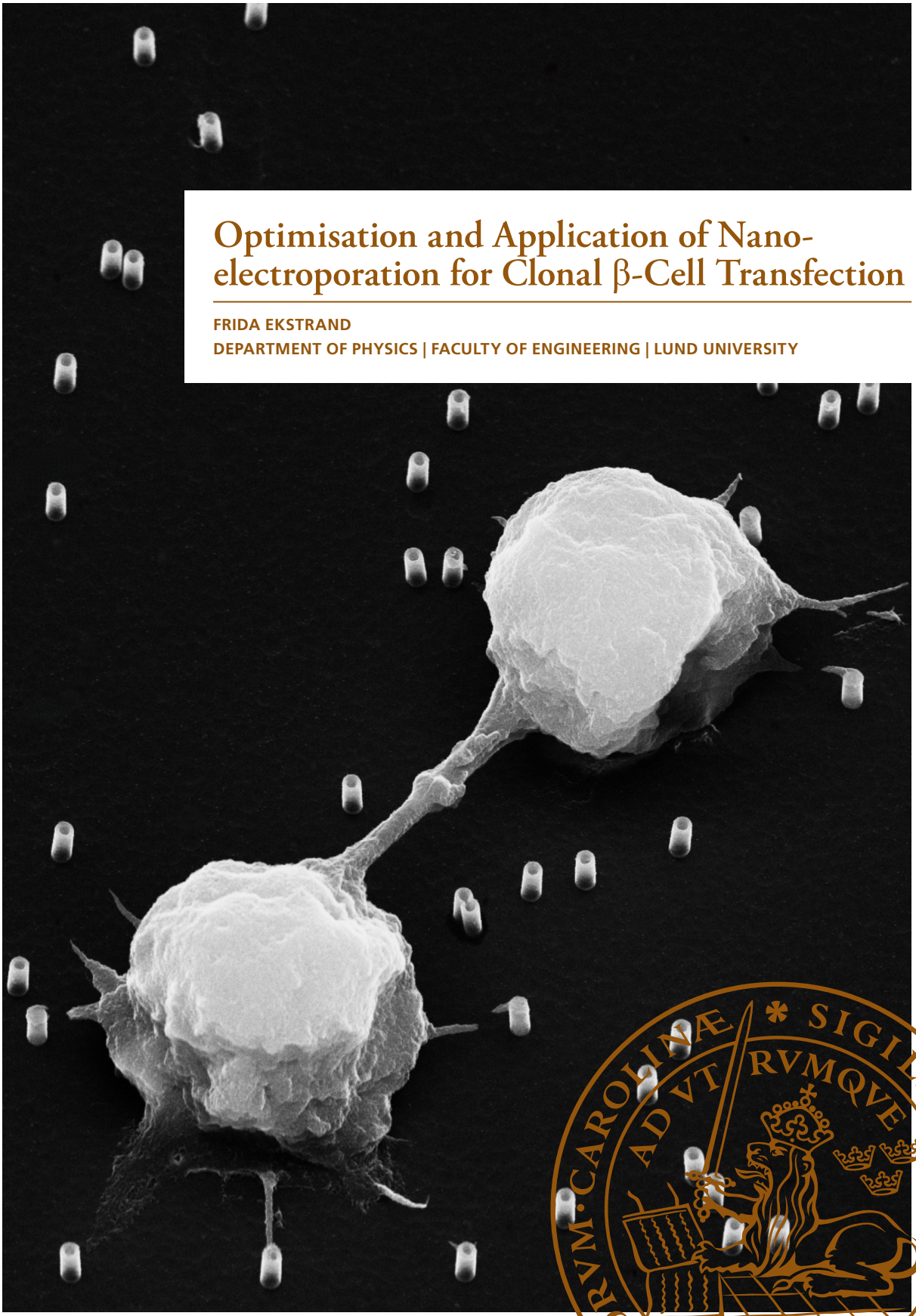

Optimisation and Application of Nano-electroporation for Clonal β-Cell Transfection

FRIDA EKSTRAND
DEPARTMENT OF PHYSICS | FACULTY OF ENGINEERING | LUND UNIVERSITY

Optimisation and Application of Nanoelectroporation for Clonal β-Cell Transfection

Optimisation and Application of Nanoelectroporation for Clonal β-Cell Transfection

by Frida Ekstrand

LUND
UNIVERSITY

DOCTORAL DISSERTATION

To be publicly defended for the degree of Doctor of Philosophy, with the permission of the Faculty of Engineering of Lund University, on Friday the 24th of October 2025 at 09:15 in Rydbergsalen, Department of Physics.

Thesis advisors

Prof. Christelle Prinz, Prof. Charlotte Ling

Faculty opponent

Prof. Mark Schvartzman

Organization	Document name
LUND UNIVERSITY Department of Physics Box 118 SE–221 00 LUND Sweden	**DOCTORAL DISSERTATION** Date of disputation 2015-10-24 Sponsoring organization
Author(s) Frida Ekstrand	

Title and subtitle

Optimisation and Application of Nanoelectroporation for Clonal β-Cell Transfection

Abstract

Within the field of cell biology, an essential tool is to deliver molecules to cells to manipulate cell behaviour and function. This enables the study of, for example, how a specific change in a cellular process contributes to a disease state. However, cells have barriers, such as the cell membrane, that need to be overcome for the molecules to have an effect. Current transfection methods, such as liposomes, viral vectors, or bulk electroporation have drawbacks such as low efficiency and cytotoxicity, which raises the need for developing new methods.

Nanoelectroporation is a gentle transfection method that induces localised electroporation in the cell membrane by applying an electric field across cells located on a substrate with nanopores or nanostraws. The localised electroporation implies that pores in the cell membrane form only where it is in contact with a nanopore/nanostraw. This provides direct access between the cytosol and the backside of the substrate, where cargo molecules are present in solution. The electric field contributes both to pore formation and increased molecular transport.

In this thesis, I have extended the use of nanoelectroporation to target clonal β-cells, insulin producing pancreatic cells. The overarching aim was to implement specific epigenetic changes to study the underlying mechanisms of type 2 diabetes. Towards this goal, I first aimed at optimising the setup for this new cell type to achieve high transfection efficiency and cell viability. The method was then applied to affect clonal β-cell insulin gene expression with an artificial transcription factor, using the CRISPR interference (CRISPRi) system. In Paper I, I optimised method parameters and demonstrated that the highest transfection efficiency for plasmids, while maintaining high cell viability, was achieved with 28 V, 2690 cells/mm^2, and MilliQ water as cargo buffer. A comparison of nanopores and nanostraws revealed a discrepancy between the transfection efficiency achieved immediately after transfection and plasmid expression 48 hours later, which could be attributed to either higher cell death or lower proliferation. This discrepancy was further investigated in Paper II, where it was found to be caused by poor cell adhesion, resulting from plasmid toxicity. Paper II also established that the substrate porosity needed to be high enough for cells to interface with a sufficient number of nanopores, that a large nanopore diameter caused higher cell death, and that an alumina surface yielded the best transfection out of the tested surface chemistries. Lastly, in Paper III, we used nanopores to inject clonal β-cells with plasmids encoding a CRISPRi system and presented a successful downregulation of insulin gene expression.

Key words

Nanostraws, Nanopores, Transfection, Electroporation, CRISPR-dCAS9

Classification system and/or index terms (if any)

Supplementary bibliographical information	Language English
ISSN and key title	ISBN 978-91-8104-679-3 (print) 978-91-8104-680-9 (pdf)
Recipient's notes	Number of pages 165 Price
	Security classification

Optimisation and Application of Nanoelectroporation for Clonal β-Cell Transfection

by Frida Ekstrand

LUND
UNIVERSITY

Cover illustration front: Clonal β-cells on a nanostraw substrate The image is acquired using a scanning electron microscope at 8500 times magnification. Thanks to Sara Davidsson Bencker for sample preparation.

Cover illustration back: Det var det bästa vi någonsin gjort.

Faculty of Engineering, Department of Physics

ISBN: 978-91-8104-679-3 (print)
ISBN: 978-91-8104-680-9 (pdf)

Printed in Sweden by Media-Tryck, Lund University, Lund 2025

Media-Tryck is a Nordic Swan Ecolabel certified provider of printed material. Read more about our environmental work at www.mediatryck.lu.se

MADE IN SWEDEN

'I solemnly swear that I am up to no good.'

- Harry Potter

Contents

Abstract

Within the field of cell biology, an essential tool is to deliver molecules to cells to manipulate cell behaviour and function. This enables the study of, for example, how a specific change in a cellular process contributes to a disease state. However, cells have barriers, such as the cell membrane, that need to be overcome for the molecules to have an effect. Current transfection methods, such as liposomes, viral vectors, or bulk electroporation have drawbacks such as low efficiency and cytotoxicity, which raises the need for developing new methods.

Nanoelectroporation is a gentle transfection method that induces localised electroporation in the cell membrane by applying an electric field across cells located on a substrate with nanopores or nanostraws. The localised electroporation implies that pores in the cell membrane form only where it is in contact with a nanopore/nanostraw. This provides direct access between the cytosol and the backside of the substrate, where cargo molecules are present in solution. The electric field contributes both to pore formation and increased molecular transport.

In this thesis, I have extended the use of nanoelectroporation to target clonal β-cells, insulin producing pancreatic cells. The overarching aim was to implement specific epigenetic changes to study the underlying mechanisms of type 2 diabetes. Towards this goal, I first aimed at optimising the setup for this new cell type to achieve high transfection efficiency and cell viability. The method was then applied to affect clonal β-cell insulin gene expression with an artificial transcription factor, using the CRISPR interference (CRISPRi) system. In Paper I, I optimised method parameters and demonstrated that the highest transfection efficiency for plasmids, while maintaining high cell viability, was achieved with 28 V, 2690 cells/mm^2, and MilliQ water as cargo buffer. A comparison of nanopores and nanostraws revealed a discrepancy between the transfection efficiency achieved immediately after transfection and plasmid expression 48 hours later, which could be attributed to either higher cell death or lower proliferation. This discrepancy was further investigated in Paper II, where it was found to be caused by poor cell adhesion, resulting from plasmid toxicity. Paper II also established that the substrate porosity needed to be high enough for

cells to interface with a sufficient number of nanopores, that a large nanopore diameter caused higher cell death, and that an alumina surface yielded the best transfection out of the tested surface chemistries. Lastly, in Paper III, we used nanopores to inject clonal β-cells with plasmids encoding a CRISPRi system and presented a successful downregulation of insulin gene expression.

Populärvetenskaplig sammanfattning

"Farbror Melker, vet du vad?
Om du inte kan skriva så att jag förstår det,
då kan du lika gärna sluta upp."

- Tjorven i Vi på Saltkråkan

Föreställ dig att du är en molekylärbiolog på väg ti... VÄNTA! Stanna kvar! Snälla? Jag förstår att det kan vara svårt (nästintill omöjligt) att föreställa sig något man kanske aldrig hört talas om. Så låt oss, i enlighet med citatet ovan, mjukstarta lite först innan vi dyker i. Som molekylärbiolog är du intresserad av processer som händer inuti celler och hur det i sin tur påverkar hur cellen fungerar. Dessa processer kan exempelvis vara hur DNA blir översatt och omvandlat till proteiner, och hur dessa proteiner gör sitt jobb. Med hjälp av denna kunskap kan man exempelvis studera sjukdomar som uppstår på grund av att någon av dessa processer inte fungerar normalt eller hur olika läkemedel påverkar cellens beståndsdelar.

Nu är vi nog redo att ta vid där vi startade. Så, föreställ dig nu att du är en molekylärbiolog på väg till jobbet en solig tisdagsmorgon. När du kommer fram tar du på dig hårnät, blå skoskydd, labbrock, och handskar - din vanliga jobbutstyrsel - och går in i labbet där ni har era celler. Du och dina kollegor jobbar med olika celltyper beroende på vad ni studerar, men du har en cellodling av något som kallas för betaceller. Detta är en typ av celler som producerar insulin i bukspottkörteln. Insulin är ett hormon som hjälper celler ta upp energi (socker) från blodet och kopplas ofta ihop med diabetes, vilket är precis den sjukdom din forskning handlar om. Typ 2-diabetes är en folksjukdom som resulterar i att man inte kan reglera sockernivån i blodet. Sjukdomen beror både på att det inte produceras tillräckligt med insulin och att celler blir mindre känsliga för insulin, vilket gör att de inte kan ta upp socker från blodet lika effektivt.

Du har ett experiment planerat så du tar ut din cellodling från inkubatorn, där de trivs i en lagom temperatur och koldioxidhalt, och slänger ett öga på dem i mikroskopet (de är tusen gånger mindre än ett knappnålshuvud, så mikroskopet är nödvändigt!). De ser ut att

må bra (Figur 1).

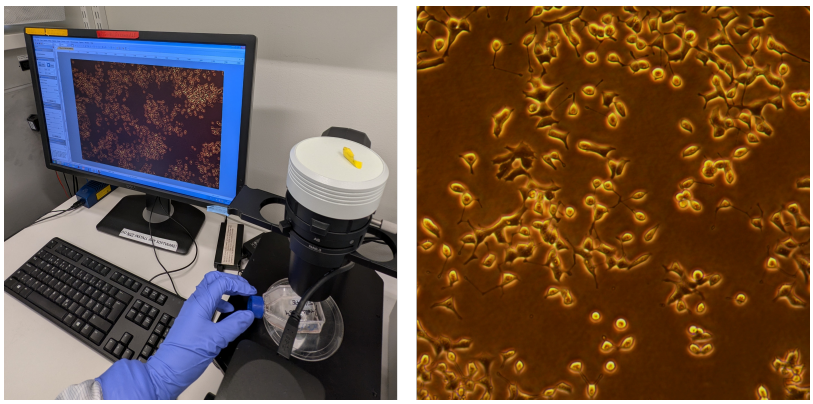

Figur 1: Du tittar på din cellodling i mikroskopet (vänster), de ser ut att må bra (höger).

Ditt experiment idag går ut på att du vill modifiera normalt fungerande celler för att efterlikna hur processerna ser ut när cellerna är sjuka. Ju mer vi vet om hur en sjukdom uppstår och ändrar cellers funktion, desto större chans har vi att hitta ett läkemedel, eller i vissa fall, till och med ett botemedel.

För att kunna modifiera cellerna behöver du få in vissa ämnen (molekyler) i dem. Dessa molekyler kan vara ganska stora (allt är relativt) och är inget cellen tar upp självmant. Det finns olika metoder för att ”tvinga” in dem i cellerna, och du funderar på vilken du ska använda. Ett sätt är att använda små fettbubblor med dina molekyler i. Eftersom membranet som omger cellen också är gjort av fett så kan bubblorna smälta samman med cellmembranet och på så sätt ta sig in i cellen. Problemet är bara att det är svårt att få ut din molekyl ur fettbubblan när den väl kommit in i cellen, vilket gör att den inte kan få den effekt du hoppas på... En annan metod är att ta hjälp av ett virus för att få in molekylerna. Då packar man in molekylerna inuti ett tomt virusskal (inget som kan orsaka sjukdom är kvar), och eftersom virus är gjorda för att ta sig in i celler (för att kunna sprida sig) så är ju det problemet löst! Men, virusskalet kan orsaka ändringar på cellens gener som du inte vill ha, och som kan ge effekter som påverkar den ändring du egentligen vill göra med din molekyl. Slutligen tänker du på elektroporering. Då har man cellerna och molekylerna flytande i en vätska, och sedan påverkar man cellmembranet med en elektrisk spänning, lite som att ge cellerna en elstöt, så att det blir små porer i det. Genom dessa porer kan sedan dina molekyler sippra in. Nackdelen med denna metod är dock att man behöver använda hög spänning, vilket gör att många celler får så stora hål att de inte kan läka ihop, och därför dör många av cellerna som man vill studera...

Gah, finns det ingen metod som är både effektiv och håller dina stackars celler vid liv!?

Det är här min forskning kommer in i bilden.

Jag har jobbat på att vidareutveckla en metod som ska kunna hjälpa till att få in molekyler i celler (specifikt har jag fokuserat på betaceller), utan att de dör av behandlingen. Denna metod kombinerar elektroporeringen som nämndes tidigare, med två typer av nanostrukturer som kan liknas vid hål eller sugrör. ”Nano” betyder enkelt nog att strukturerna är väldigt små - de har en bredd som är tusen gånger mindre än tjockleken av ett hårstrå. För att göra våra nanostrukturer utgår vi från ett plastmembran med många små porer (20 miljoner på en yta som är 1x1 cm) som går rakt genom membranet, så det blir som små rör från ena sidan till den andra. Dessa bearbetar vi så att vi antingen får en yta med nanoporer, fortfarande platta hål men med ett annat ämne (aluminiumoxid) på ytan, eller så att det bildas nanostrån, rör som sticker upp från ytan (också gjorda av aluminiumoxid).

För att utföra ett experiment så lägger vi cellerna på nanoporerna/stråna (se skiss i Figur 2) och så har vi en vätska med våra molekyler i under plastmembranet. När cellerna bara ligger där så är deras cellmembran helt, men när vi startar en elektrisk spänning så kommer det få små hål i sig. Skillnaden från elektroporeringen som nämndes tidigare är att spänningen kommer koncentreras enbart till öppningen av nanoporerna/stråna, istället för att påverka hela cellen. Det betyder att en lägre spänning är tillräcklig för att åstadkomma hålen i cellmembranet, och dessutom blir det bara hål precis ovanför nanopor/stråöppningen. Den elektriska spänningen hjälper dessutom till att dra molekylerna (som har en viss laddning) från undersidan av plastmembranet, genom hålen, och in i cellen på ovansidan.

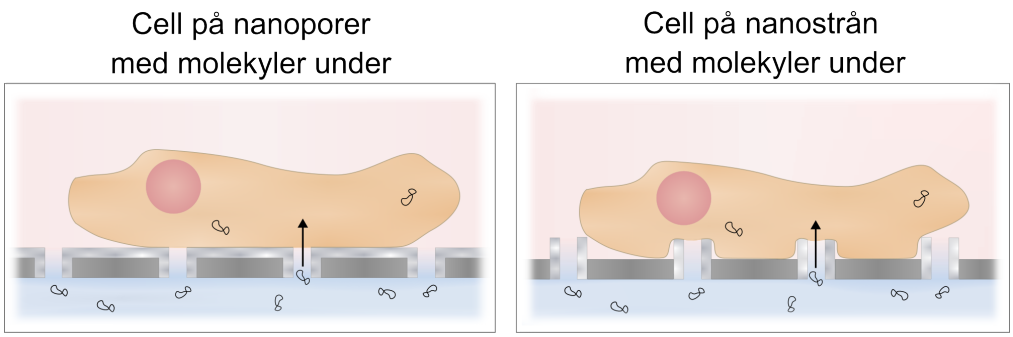

Figur 2: Cell med cellkärna på nanoporer till vänster och nanostrån till höger. De mörkgråa fälten symboliserar plastmembranet, det melerade gråa är aluminiumoxid, och ljusblått är vätskan med molekylerna (svarta former) i. Bilderna är inte skalenliga.

I min forskning har jag optimerat flera delar av denna metod för att den ska kunna användas optimalt på betaceller. I mitt första projekt fokuserade jag på delar relaterade till elektroporeringen, så som densiteten av celler och hur stark spänningen bör vara. Här kom jag bland annat fram till att celldensiteten inte kan vara för hög eftersom cellerna då hamnar ovanpå varandra och många celler inte kan bli injicerade med några molekyler, men även att valet av en ”lagom” spänningsnivå är en balansgång mellan att hålla celler vid liv och att få in molekyler i så många celler som möjligt. Dock såg vi också att det kanske inte

nödvändigtvis är hög spänning som gör att celler dör av behandlingen. Med högre spänning dras fler molekyler in i cellen, och som med så mycket annat så är ”för mycket” inte hälsosamt.

I mitt andra projekt undersökte vi hur variationer i plastmembranet och nanoporerna/stråna påverkade hur många celler som mottog molekyler. Vi testade bland annat olika typer av ytmaterial, varierade även hur tätt det var med nanoporer på ytan, och jämförde nanoporer med nanostrån. Vi kom fram till att nanostrån gjorde att fler celler fick molekyler, jämfört med om man använde nanoporer. Tyvärr var det också fler celler som dog när man använda nanostrån, men precis som tidigare kan detta ha berott på att det drogs in för mycket molekyler i cellerna. Detsamma gällde när vi testade att använda nanoporer med större diameter - fler celler dog av de större hålen.

Slutligen, i mitt tredje projekt så försökte jag, tillsammans med forskare på Diabetescenter i Malmö, använda specifika molekyler för att ändra hur mycket insulin betacellerna bildade. Dessa molekyler ändrade ingenting i cellens genetik, utan påverkade i stället hur mycket genen i fråga översattes till protein i cellen. En del av de processer som reglerar hur mycket en gen översätts (genuttryck), utan att ändra genen i sig, kallas för epigenetik (”över genetiken”), och har setts vara en bidragande faktor i vissa sjukdomar, däribland diabetes. Molekylerna som behövs för detta är stora och svåra att få in i cellerna med de vanligaste metoderna. Men, med nanoelektroporering har vi lyckats få in liknande molekyler i cellerna och sett en minskning i insulinproduktionen. Även om de molekyler vi använde här tekniskt sett inte ger en epigenetisk förändring så är det ett första steg mot det, och ett steg i rätt riktning för att kunna studera epigenetikens roll inom diabetes på ett nytt sätt.

Popular science summary

"Uncle Melker, you know what?
If you can't write so that I understand it,
then you might as well stop."

- Tjorven from Seacrow Island

Imagine that you are a molecular biologist on the wa... WAIT! Stay! Please? I realise that it can be tough (almost impossible) to imagine something that you might never have heard of. So let us, in line with the quote above, learn to walk before we run. As a molecular biologist, you're interested in processes that happen inside cells and how those, in turn, affect how the cell functions. These processes can, for example, be how DNA is translated and turned into proteins and how these proteins do their jobs. With this knowledge, it is possible, for instance, to study diseases that occur when some of these processes don't function normally or how different drugs affect the cell's constituents.

Now I think we're ready to resume where we started. So, imagine you are a molecular biologist on the way to work on a sunny Tuesday morning. When you get there, you put on a hair net, blue shoe covers, lab coat, and gloves - your typical work attire - and enter the lab where you have your cells. You and your colleagues work with different cell types depending on what you study, but you have a cell culture of something called beta cells. This is a type of cell that produces insulin in the pancreas. Insulin is a hormone that helps cells take up energy (sugar) from the blood and is often associated with diabetes, which is precisely the disease your research is about. Type 2 diabetes is a public health issue that results in a loss of the ability to regulate the blood sugar level. It is caused both by a lack of insulin production and that cells becomes less sensitive to insulin and hence can not take up sugar from the blood as efficiently.

You have an experiment planned, so you take out your cell culture from the incubator, where they thrive in a suitable temperature and carbon dioxide concentration, and have a quick look at them in the microscope (they are a thousand times smaller than a pinhead,

so the microscope is necessary!). They look like they are doing well (Figure 1).

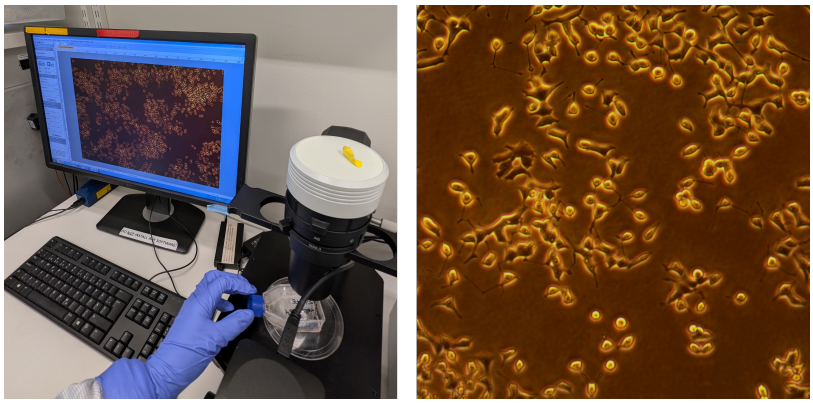

Figure 1: You look at your cell culture in the microscope (left), they look good (right)

Your experiment today centres around modifying normal-functioning cells to mimic how the cellular processes behave when cells are sick. The more we know about how a disease arises and how it alters cell function, the greater chance we have to find a medicine or, in some cases, even a cure.

To be able to modify your cells, you need to get certain substances (molecules) into them. These molecules can be rather big (everything is relative) and are not something the cell incorporates voluntarily. However, there are several ways to 'force' the molecules into the cells, and you are contemplating which one to use. One way is to use tiny bubbles of fat surrounding your molecules. Since the cell membrane is also made of fat, the bubbles can merge with the cell membrane and, in that way, enter the cell. The problem is that it is hard to get your molecules out of the bubbles when they are located inside the cell, which means they can not cause the effect you are after... One can also use viruses to help the molecules inside the cells. Then, the molecules are enclosed in an empty virus shell (nothing that can cause disease is left). Since viruses are naturally good at getting into cells (to multiply and spread), that problem is solved! However, this method can cause changes in the cell's genome that you don't want, which can give effects that interfere with the change you want to achieve with your molecule. Finally, you're contemplating electroporation. Here, the cells are suspended in a liquid with the molecules, and the cell membrane is affected by applying an electric potential, sort of like giving the cells an electric shock. The potential induces the formation of pores in the cell membrane where the molecules can seep in. The drawback with this method is that since you need such a high electric potential, many cells get large pores that can't heal, and therefore, many of the cells you want to study, die.

Argh, aren't there any method that is both efficient and keep your poor cells alive!?

This is where my research comes into the picture.

I have worked on further developing a method that will aid in getting molecules into cells (specifically, I have focused on beta cells) without them dying from the treatment. This method combines electroporation, which was mentioned previously, with two types of nanostructures that either resemble holes or straws. 'Nano' plainly means that the structures are really tiny, with a width a thousand times smaller than the thickness of a human hair. To make our nanostructures, we starts with a plastic membrane with many tiny pores - 20 million on an area of 1x1 cm - that go straight through the membrane, like small pipes from one side to the other. These membranes are then processed so that the surface either contains nanopores, still holes but with another material (aluminum oxide) on the surface, or nanostraws, small pipes that stick up from the surface (also made of aluminum oxide).

For an experiment, we lay the cells on the nanopores/straws (see sketch in Figure 2), and have a liquid with our molecules on the other side of the plastic membrane. When the cell is just lying there, its cell membrane is intact, but when we apply an electric potential, small holes will form in it. The difference to the electroporation mentioned earlier is that the potential will concentrate to the opening of the nanopores/straws instead of affecting the whole cell. This means that a lower electric potential can achieve holes in the cell membrane and that they will only open straight over the nanopore/straw openings. The electric potential also helps drag the molecules (which are charged) from under the plastic membrane, through the holes, and into the cells on top of the plastic membrane.

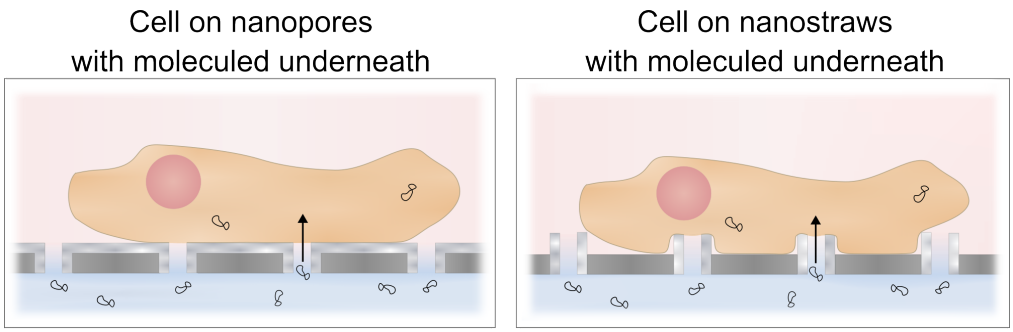

Figure 2: Cell with nucleus on nanopores to the left and nanostraws to the right. The dark grey areas represent the plastic membrane, the lighter grey layers are aluminum oxide, and light blue is the liquid with molecules (black shapes).

In my research, I have optimised several parts of this method for it would work optimally on beta cells. In my first project, I focused on parts related to electroporation, such as the density of cells and how strong the potential should be. We concluded, among other things, that the cell density can not be too high since the cells start stacking on top of each other and thus many cells can not be injected with any molecules, but also that choosing

the right potential means to balance keeping cells alive and getting molecules into as many cells as possible. Although, we also saw that it might not be the high potential that kills the cells. With a higher electric potential, more molecules are pulled into the cell, and as with many other things, 'too much' is not healthy.

In my second project I investigated how variations in the plastic membrane and nanopores/straws affected how many cells received molecules. For example, we tested different surface materials, varied how many nanopores/straws there were on the surface, and compared nanopores with nanostraws. We determined that nanostraws resulted in more cells receiving molecules, in comparison to when using nanopores. Unfortunately, more cells also died. But just as previously, this could be because too much molecules were dragged into the cells.

Finally, in my last project, I, together with researchers at Diabetes Centre in Malmö, used specific molecules to change how much insulin the beta cells produce. These molecules did not change anything in the cell's genetics but instead affected how much the gene in question was translated into protein in the cell. A portion of the processes that regulate how much a gene is translated (gene expression) without changing the gene itself is called epigenetics ('over genetics'), which is a factor in certain diseases, diabetes, among others. The molecules needed for this are big and difficult to get into the cell using the most common methods. With nanoelectroporation, we managed to inject very similar molecules and saw a reduction in insulin production. Although these specific molecules were not technically altering the epigenetics, it was a first step towards it and a step in the right direction for studying the role of epigenetics in diabetes in a new way.

Acknowledgements

As I near the end of this PhD journey, it is crystal clear that this has been far from a solo mission. With a lot of help and support, I have finally made it here, capping off what has somehow become over 11 years of university life. There's been a fantastic group of people who kept me going, and I will now attempt a seemingly impossible mission: squeezing all of you into just a few pages.

Firstly, Christelle, thank you for all the time and support you have given me over these 5.5 years. I must say, at the time, I was a bit surprised that you agreed to see me in the middle of summer to discuss a possible master's project, not due to start until a good six months later. Your eagerness was contagious, and since I prioritised the choice of supervisor over project (fortunately, you presented very cool stuff as well), I decided I didn't need to look any further - a choice I have never regretted. Most times, even when I thought the results were... let's say... not the most promising, you managed to find the positive side of things, and I have always left our meetings in better spirits than when I entered. You have been truly invaluable.

To my first co-supervisor, Diogo, without your enthusiasm and love for science during my master's project, I'm not so sure I would have ended up on this path. I really wish you were still here to see this journey through to the end. At least we didn't give up on the project you started, even though it seemed impossible at times, and it's now (at least in my opinion) the coolest part of my thesis. I have kept the short message you left on the whiteboard outside the lab during your last visit. It's not much, but it makes me smile. Charlotte, you stepped in as co-supervisor without hesitation when Diogo wasn't able to continue. The knowledge you shared in meetings, comments, and feedback has been essential for writing this thesis. Thank you.

Therese, I think our time spent in corridor-C200-meetings exceeded reason at times, but that's what it took to keep us sane! I really appreciate your friendship and all the support and help you have gladly given me throughout this journey. Soon, both of us will have left FTF, but the asbestos hood remains...Oh well. Thea, thank you for all the fun conversations, jigsaw sessions, and corridor meetings (this group is good at those!) over these past few

years. You always go out of your way to help and make sure everyone around you is feeling well. It's a blessing to be around someone like that. Sara, I couldn't have asked for a better master's student. You picked things up so quickly that we could move on from being teacher and student to colleagues and friends in no time, and I'm so happy for that. To the rest of the current and previous Prinz group members: Yupeng, Mirella, Pedro, Sabrina, Mokhtar, Karthik, Mercy, Elke, and Martin - your input and expertise have taught me a lot, and I appreciate all the laughter we managed to squeeze in along the way!

To the biowaste crew, thank you for all the derailed meetings and for always being willing to help whenever possible. It has been wonderful (and a good exercise in patience) to hear us veer off from the agenda of practical lab discussion to instead debating ethical considerations of... something (I can't even remember), all while someone desperately tried to get us back on track.

I want to send a collective big thank you to all of my fellow PhD students and post docs at FTF - no one named, no one forgotten (because that was my biggest fear when writing this). We've had so much fun and laughed so much that I'm convinced it has added years to my life. The retreats, after works, cooperative solitaire games, work out sessions, and weird lunch discussions have all been a blast. While everyone contributed to these fun times, there are a few people who, to me, are deserving of a little bit of extra attention. Linnéa, for being the partly unwilling yet self-appointed event planner who never loses. Your door has always been open (otherwise I let myself in), and you have brightened many of my days by just being you. Max, for pushing us all to be more fit, both by 'forcing' us to come to HIT with you and for always offering to relieve us of our Friday fikas. When you are around, FTF is a much livelier and more fun place to be. Julia, for being a force of kindness and laughter everywhere you go. You always take the time to greet people with their names, even if you are in the middle of a conversation, leaving everyone feeling noticed and welcome. Lastly, Thanos and Matteo, thank you for making the tiny office in the C200-corridor seem bigger than it was.

This journey would have been impossible without the help of the FTF administrative and supporting staff. Thank you to Anastasiia and Alexandra for having a solution to almost any problem and arranging fika every week! (I don't think you can ever get enough cred for that), The LNL staff for being so fast in fixing any issue I encountered in the clean room, Adam for ensuring all PhD students were on track and feeling well, and Dan for fostering such a great atmosphere at FTF. I was also fortunate to have great collaborators outside of FTF. Sabrina and Karl, I have learned a lot from you about a field far outside my background, and I really appreciate your patience. Also, thank you Zippo for always taking time out of your busy day to help me fetch dry ice when I needed it.

PO and Johan, where do I even begin? You have given me so much, not just an incredibly cool job and countless great memories from all sorts of places, but also some of my closest

friends (don't worry, I'll come back to you). Going from hating public speaking in high school to performing Physics and Lasershows, goofing around on stage in front of 800 people... that's something I never imagined myself capable of. Over these 10 (!!) years, I have learned and experienced so much that I will carry with me for the rest of my life - all because you saw something in me during that short week in 2014. Thank you, so, so much.

To all the people I have worked with in the Physics and Lasershow - we have worked long hours, to say the least, but with you, it has always felt like a privilege. An extra warm hug to 'the old gang': Vasse, Daniel, Jonas, Alex, David, AMes, and Elin. All those hours spent together have made us into a well-oiled machine, and I don't think I know any other group of people who can switch into 'efficiency mode' so wholeheartedly when needed. As you are (perhaps painfully) aware of by now, I *love* organisation and efficiency, so naturally, this is why I love you. Just kidding, of course (but it doesn't speak against you). I love you because you are amazing people, because we always manage to have fun (even when running on fumes during our 19th working hour), and because challenges like Montenegro, Serbia, and Växjö simply forged us together.

To the people who made my first years (and beyond) in Lund a fantastic period: Rebecca, Charlie, Eric, and Nycklis. I look back at our time in Rydbergs, both struggling to understand physics and drinking a lot of beer, with great fondness. Without you it would have been much, much, harder to make it past the first years. Thank you for all the great times. Also thank you to the rest of the Schlagerklubb-and-brunch gang: Emil, Charlotte, Simon, Johanna, David, Linnéa, Veronica, and surely some that currently slipped my mind.

Thank you to all my cool and inspiring instructor colleagues at Gerdahallen for making the gym such a great place to be, both in your classes and in the changing room. Emmy, our constant yapping has made me miss the bus on more than a few occasions, but I don't mind. To others, it might sound like we complain a lot about mammoths and stuff, but who can really blame us? Thank you for befriending 'Wilma's old, old sister', I've had a lot of fun.

The biggest thanks to my family - Mom, Dad, Cajsa, and Wilma - for sparking my curiosity about the world from the very start (the fact that sugar contains carbon is quite literally burnt into my memory), for 'forcing' me to move forward when I was stuck, and for always being there with support and encouragement. It means the world to me. Even better, you also happen to be a tad crazy and absolutely hilarious to be around. Let's just put it in print: our table always has the most fun at restaurants. Laugh on three?

While on the subject of home, there are a few more incredible women I have to mention: Amanda, Andréa, Annie, Erica, Julia, and Sallie. Thank you for sticking by me and for making a genuine effort to remember what on earth you are supposed to say when someone asks, 'So, what is Frida doing these days?', I know that hasn't been easy. We might not hang out as often as we used to or want, but we've been through so much together at this point

that I think we're pretty much stuck with each other for life, and I wouldn't have it any other way.

Lastly, David (I guess there's one more thing to thank PO and Johan for), I'm so glad we have done this long journey together. Being a PhD-student is tough, but being able to come home, complain to, and discuss with someone who knows exactly what you're going through makes it a whole lot easier. You're my biggest supporter, the one who tolerates my alleged hanger and my impulsive projects, and the one I can rely on to make sure I actually relax once in a while (I know it isn't always the easiest task). I love you, and thank you for everything, truly. As we now finally 'finish school', we may not get to literally fly off in a cascade of fireworks (although, I did draw us some), but the sentiment remains the same:

'I think we've outgrown full-time education ...
Time to test our talents in the real world, d'you reckon?'

- Fred Weasley

List of publications

This thesis is based on the following publications, referred to by their Roman numerals:

I **Achieving efficient clonal beta cells transfection using nanostraw/nanopore-assisted electroporation**
F. Ekstrand*, M. Mapar*, S. Ruhrmann, K. Bacos, C. Ling, C.N. Prinz
RSC advances, 14, 22244 (2024)

*These authors contributed equally

I fabricated the nanostraw/nanopore substrates, conducted experiments for the effect of voltage, cell density, and the comparison between nanopores and nanostraws. The experimental results regarding the effect of buffer conductivity was a joint effort between me and M. Mapar. I was main responsible for writing of the paper, together with C.N. Prinz.

II **Plasmid-induced cytotoxicity revealed by nanopore and nanostraw electroporation**
F. Ekstrand, S. Davidsson Bencker, Y. Yang, S. Ruhrmann, C. Ling, C.N. Prinz
Nanoscale (2025)

The results in this paper was a joint effort between me and S. Davidsson Bencker. I have done experiments to complement the data about the surface chemistry, both regarding transfection efficiency and phase holographic imaging. I also produced the result for comparing nanopores with the two types of nanostraws, as well as for the investigation of why GFP expression was lower than expected. I wrote the manuscript together with C.N Prinz.

III **Nanopore Electroporation: A new delivery method within the field of epigenetic editing**
F. Ekstrand*, S. Ruhrmann*, K. Bacos, S. Bartel, P. Jellema, M. Rots, C. Ling, C.N. Prinz
In preparation

*These authors contributed equally

I fabricated the nanopore substrates and conducted experiments for optimising voltage and pore diameter. The results for modifying gene expression was a joint effort, where I did the transfection using nanopore electroporation, while S. Ruhrmann performed the qPCR analysis. I wrote the manuscript together with co-authors.

All papers are reproduced with permission of their respective publishers.

Publications not included in this thesis:

Monitoring the Intracellular Fate of Molecular Beacons: The Challenge of False Positive Signals
D. Volpati, P.H.B. Aoki, T.B. Johansson, R. Munita, F. Ekstrand, S. Ruhrmann, K. Bacos, C. Ling, C.N. Prinz
Advanced NanoBiomed Research, 4, 2300147 (2024)

Enhancing Photothermal Therapy Against Breast Cancer Cells by Modulating the End Point of Gold-Shell-Isolated Nanoparticles Using Nanostraw-Assisted Injection
S.A. Camacho, P.H.B. Aoki, F. Ekstrand, O.N. Oliveira Jr., C.N. Prinz
ACS Applied Materials & Interfaces, 17, 27816 (2025)

Acronyms

ALD atomic layer deposition

cDNA complementary DNA

DNA deoxyribonucleic acid

EDL electric double layer

EOF electro-osmotic flow

FSC forward scatter

GFP green fluorescent protein

ICP-RIE inductively-coupled plasma reactive ion etching

kbps kilobase pairs

mRNA messenger RNA

NED No Effector Domain

PAM protospacer adjacent motif

PC polycarbonate

PVP polyvinylpyrrolidon

qPCR quantitative polymerase chain reaction

RNA ribonucleic acid

SEM scanning electron microscope

sgRNA single guide RNA

siRNA silencing RNA

SKD Super Krüppel-associated Box Domain

SSC side scatter

Chapter 1

Introduction

Diabetes, a group of diseases impairing the ability to regulate the blood glucose level, is affecting around 589 million people's lives today and is expected to increase further [1]. These diseases are hereditary, but genetics is not the only contributing factor to their heritability [2]. The onset of type 2 diabetes, a disease characterised by impaired function of the insulin-producing cells in the pancreas (β-cells) in combination with insulin resistance in the target tissues, is strongly affected by environmental factors and lifestyle [3]. These factors can induce hereditary chemical changes to the genome, known as epigenetic modifications, without altering the genetic code itself. Epigenetic modifications can, in turn, affect cell function. Indeed, differences in the epigenome have been observed between patients with type 2 diabetes and non-diabetic controls [4]. However, whether the disease causes the epigenetic changes or vice versa is yet to be better determined.

To study cellular changes, both genetic and epigenetic modifications can be induced in cells by delivering particular molecules to their cytosol (fluid part of the cell interior, not including organelles). In terms of diabetes, an efficient and safe delivery method would not only enable the study of specific molecular changes in β-cells to advance the understanding of the disease development, but could also open the possibility of altering cells for therapeutic purposes. This thesis work has taken some tentative first steps towards that ultimate goal.

Delivering molecules to cells can be done by utilising viruses, lipid-based nanoparticles, and bulk electroporation. However, using viruses has raised safety concerns, and using lipid-based nanoparticles or bulk electroporation results in low cell viability; therefore, new delivery methods are needed. The aim of these past five years of research, summarised in this thesis, has been to contribute knowledge about how insulin-producing cells can be gently injected with molecules intended to alter cellular behaviour or function, utilising a method that, to our knowledge, has not yet been used on this cell type. This method,

nanoelectroporation, entails applying an electric field across cells lying on a substrate that contains nanoscale channels, to form pores in the cell membrane (cargo molecules are in solution on the backside of the substrate). The nanochannels focus the electric field so that it only affects the area of the cell membrane in contact with the nanochannel openings, making it a gentle method that maintains high cell viability. After pores in the cell membrane have been opened, the electric field aids the transport of charged cargo through the nanochannels, making the delivery more efficient. The work contributes to a fundamental understanding of how various method parameters affect cells and transfection efficiency and offers a glimpse into possible future applications in diabetes research.

1.1 Outline

The next chapter of this thesis, named **Background** (Chapter 2), summarises relevant basic concepts in biology and physics, puts the work into context, and conveys its importance. Chapter 3 introduces the **Experimental methods** used to explore nanoelectroporation as a transfection method for clonal β-cells. Descriptions of how these methods work and their application within the frame of this thesis work will be provided. Apart from how to handle cells and carry out nanoelectroporation, it also dives into how to fabricate the nanosubstrates and the methods used to analyse cells. When familiarised with the background and methods, my work on **Optimisation of nanoelectroporation transfection parameters** (Chapter 4) for clonal β-cells is presented. Outlined first is the work on optimising parameters related to the electroporation (**Paper I**), and then the study of how nanosubstrate parameters affect cells and results (**Paper II**). After optimising the system, Chapter 5, **Modification of gene expression using nanoelectroporation**, presents how we have utilised nanoelectroporation to modify the expression of insulin in clonal β-cells (**Paper III**). Lastly, in **Conclusions and outlook** (Chapter 6), the results are summarised, and a reflection on potential future work is provided.

Chapter 2

Background

2.1 Proteins and their synthesis

Eukaryotic cells (cells with a defined nucleus) are complex, with a variety of compartments and molecules with specific functions that need to be in balance; the genome needs to be copied and used correctly, the organelles need to function, nutrients need to be converted, and waste needs to be expelled, to mention a few. At the heart of all these cell functions lie proteins, molecules that each have distinct tasks, ranging from catalysing reactions to providing structural stability to cells. All the proteins that a specific cell needs (and even more that it has the potential to produce) are encoded in the genome and constructed from building blocks called amino acids, arranged in a unique sequence determined by the protein's corresponding gene sequence.

Going from a gene to a protein, termed gene expression, requires two subsequent mechanisms to occur: transcription and translation. Transcription is the process of copying the gene sequence from the deoxyribonucleic acid (DNA) in the cell nucleus into ribonucleic acid (RNA). For transcription, the enzyme RNA polymerase binds to the DNA, opens the double strand, and synthesises the RNA with one of the DNA strands as a template. If the synthesised RNA encodes a protein, it is called a messenger RNA (mRNA). When transcription is complete, the second process, translation, can take place. For that, the mRNA is transported out of the nucleus to a ribosome in the cytosol. Ribosomes are the protein factories of the cell and translate the mRNA into a chain of amino acids. During or after translation, the chain of amino acids folds into a functional protein that can then perform its specific task in the cell. Normal cell function does not rely solely on a correct genetic code and accurate progression of transcription and translation (so that all proteins are working as intended), but also on how much of a particular protein is produced and

when. An abnormality in any of these factors can be related to disease states, such as cancer [5] and diabetes [6].

To study cellular changes related to diseases like these, an essential technique is to introduce chosen molecules into cells, known as intracellular delivery. With this, it is possible to manipulate cells in a controlled way and study specific changes in, among other things, proteins.

2.2 Investigating disease-causing mutations with CRISPR-Cas9

Intracellular delivery of the genetic editing tool CRISPR-Cas9 (Clustered Regularly Interspaced Short Palindromic Repeats - CRISPR-associated protein 9) enables precise modifications of the genome [7], and its discoverers were awarded the Nobel prize in 2020 [8]. The research fields of genetic mutations and genetic editing are beyond the scope of this thesis; therefore, I will only briefly introduce the working principle of CRISPR-Cas9 here, as it will become relevant later.

The CRISPR-Cas9 tool consists of two molecules, a single guide RNA (sgRNA) and a Cas9 protein, see Figure 2.1. The sgRNA is complementary to a target sequence on the DNA, while Cas9 is a nuclease (enzyme that breaks the links between nucleic acids) that binds to the DNA and can cut both strands. These two molecules form a complex, a ribonucleoprotein, that reads the DNA until it finds a sequence called protospacer adjacent motif (PAM). It then opens the double strand and checks if the sgRNA matches the neighbouring gene sequence. If so, the complex binds, and the Cas9 cleaves both strands in that location. If not, the complex moves on until the following PAM sequence and the procedure is repeated.

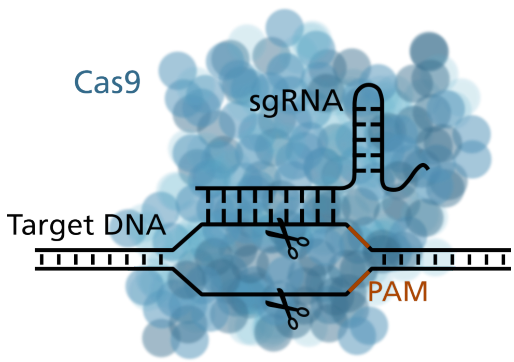

Figure 2.1: Schematic of the CRISPR-Cas9 genetic editing tool. The Cas9 and sgRNA form a complex, which binds to the target DNA. The complex reads the DNA and opens the double strand when reaching a PAM sequence. If the sgRNA is complementary to the neighbouring DNA sequence, the complex will bind to that location and cut both DNA strands.

CRISPR-Cas9 can help uncover knowledge about diseases caused by mutations, by either inducing them or correcting them. The latter also suggests that it can be used in therapeutics to treat genetic errors in various diseases [9]. However, gene expression can also be affected by factors other than the genetic code. Two of the mechanisms responsible for regulating the rate of gene expression are transcription factors, proteins that bind to specific locations on the genome to regulate the transcription rate of the downstream gene, and the epigenome.

2.3 The epigenome

The epigenome, literally meaning 'above the genome' in Greek, is a collection of molecular modifications that do not alter the DNA sequence of the genome but attach chemical compounds in specific places on the DNA to promote or inhibit the expression of a particular gene [10]. While the DNA sequence is the same for all cell types within an individual, the epigenome varies between cell types, which ensures cells produce only the proteins necessary for their specified function. That results in the very different appearance and function between cell types and tissues

One type of epigenetic mark is the attachment of methyl (CH_3) groups to DNA or histones, the proteins involved in DNA packing. There are around 2 metres of DNA in a human cell nucleus (5-10 µm in diameter), so it needs to be well-organised [11]. For an overview of the organisation of DNA in the cell nucleus, see Figure 2.2. Histones form cylinder-shaped nucleosomes that the DNA wraps around. The nucleosomes bundle into a chromatin fibre that, in turn, folds into a chromosome. More details on epigenetic modifications and their effect will be discussed in later sections.

The epigenome has been found to play a role in several diseases [12, 13, 14, 15], with epigenetic differences identified in cells from healthy and diseased people. While the genome is relatively static in an individual, over the course of a lifetime, a person's environment and lifestyle can impose changes in the epigenome [12]. Those changes can, in some cases, be associated with disease states, and as epigenetic changes can be inherited, they may also affect future generations. There are indications of epigenetic modifications being involved in both type 1 and type 2 diabetes, as genetics can only explain parts of the disease heritability, meaning other mechanisms must be at play as well [3]. Being able to investigate the effects of specific epigenetic changes could expand our understanding of disease mechanisms and increase the potential for drug development [16]. Additionally, due to the reversible nature of epigenetic marks, the ability to change the epigenome could help treat unfavourable epigenetic traits. To study these particular epigenetic changes in a controlled environment, they ought to be induced in the cell in a reliable manner, which can be achieved using the CRISPR-dCas9 system.

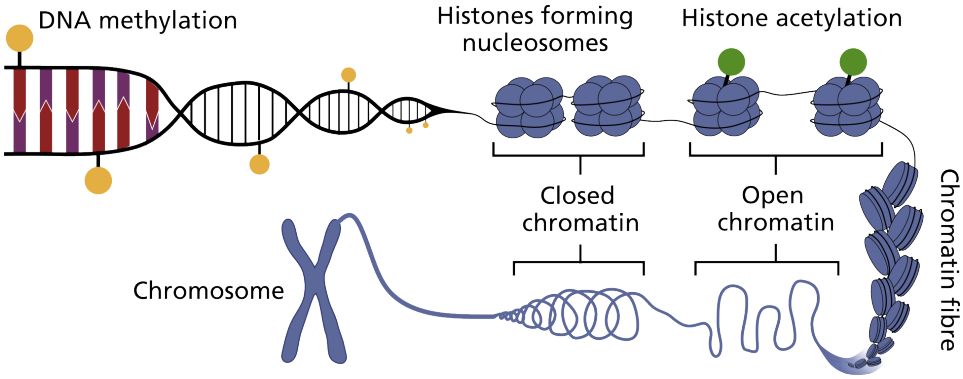

Figure 2.2: Schematic of the organisation of chromosomal DNA and two types of epigenetic markers, DNA methylation and histone acetylation. Starting from the top left, DNA can be methylated (attachment of a methyl group), which can inhibit RNA polymerase from binding. The DNA strand wraps around eight histones, which together form a nucleosome, and the nucleosomes are packed tightly into a chromatin fibre, which folds into a chromosome. Histones can be acetylated, which invokes a conformational change, resulting in a more open chromatin structure that, in turn, promotes transcription.

2.4 Modification of gene expression using CRISPR-dCas9

The extra 'd' in CRISPR-dCas9, compared to CRISPR-Cas9, stands for 'dead', meaning that the protein has been modified to be catalytically inactive, no longer able to cleave DNA. Instead, other molecules can be bound/added to dCas9, such as artificial transcription factors or epigenetic modifiers [15], both able to influence gene expression, as further explained below.

Artificial transcription factors are molecules that bind to a specific DNA sequence and directly affect gene expression with a regulatory domain, which can either inhibit or promote gene expression. These molecules are synthetic, but mimic the function of natural transcription factors that are normally present in the cell. When an artificial transcription factor that down-regulates gene expression (repressor) is added to the dCas9 complex (see Figure 2.3), the system is called CRISPR interference (CRISPRi). The added repressor recruits other proteins that together suppress the expression of the target gene by directly inhibiting RNA polymerase from binding and/or by closing the chromatin structure.

Epigenetic modifiers are enzymes that also affect gene expression but through other mechanisms. When epigenetic modifiers are fused with CRISPR-dCas9, these complexes can achieve chemical changes to DNA or histones, such as attaching or removing methyl or acetyl ($COCH_3$) groups (see figure 2.2), in selected locations with high precision. For instance, attaching methyl groups (methylation) to the RNA polymerase binding site inhibits transcription [16], whereas de-methylation stimulates gene expression. These modifications can be achieved with, for example, DNA methyltransferases (DNMTs) and Ten-eleven

translocation enzymes (TETs), which can methylate and demethylate the binding sites, respectively. DNA methylation in other parts of the genome can be either positively or negatively associated with gene expression, depending on the genomic location [12]. Attaching methyl groups to histones also affects gene expression, and can both inhibit and promote expression, depending on the placement of the methyl group on the histone. Acetylation (attachment of an acetyl group) of the histones can lead to conformational changes in the chromatin (also depending on the exact location), resulting in a more open structure that promotes transcription (see Figure 2.2), whereas deacetylation inhibits it (closed structure) [16].

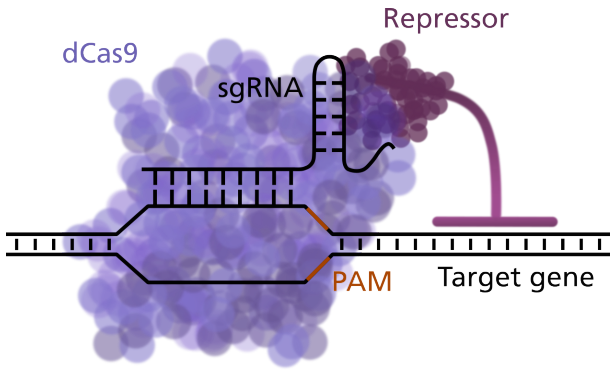

Figure 2.3: Schematic of the CRISPRi system. A repressor and sgRNA bound to dCas9 form a complex which binds to the sgRNA complementary sequence. The complex reads the genome and opens the double-stranded DNA when it reaches a PAM sequence. If the sgRNA is complementary to the neighbouring DNA sequence, the complex will bind to that location, which is close to the target gene. The attached repressor hinders transcription by attracting other inhibiting proteins.

2.5 CRISPR-complexes can be delivered to cells in three formats

When delivering CRISPR complexes to cells, three formats are available: DNA (in the form of plasmids), RNA, or ribonucleoprotein - all with their strengths and weaknesses. Plasmids require the most processing and transport within the cell after delivery; therefore, they will serve as the starting point of this section.

The term plasmid was first coined in the 1950s as any DNA distinct from the chromosomal DNA [17]. They are double-stranded circular (on rare occasions linear) DNA molecules commonly found in bacteria that are processed independently from the chromosomal DNA in the cell. However, plasmids can nowadays also be artificially produced. The artificially made plasmids (which will hereafter be denoted simply as 'plasmids') are often designed to contain one or several genes of interest. To utilise them, the cell machinery needs to express the plasmid after it has entered the cell. For a schematic of this process, see Figure 2.4.

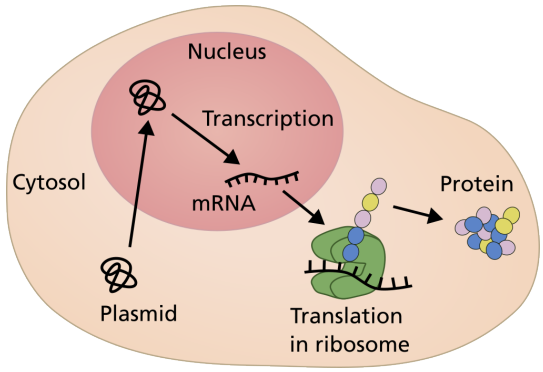

Figure 2.4: Overview of the cellular processing of a plasmid after it has entered the cytosol. It relocates to the nucleus during cell division, after which it is transcribed from DNA to mRNA. The mRNA then returns to the cytosol, where it is translated into a string of amino acids by a ribosome, and the string then folds into a functional protein.

As a plasmid enters the cell and is present in the cytosol, it needs to first relocate to the nucleus. The nuclear envelope consists of an inner and an outer lipid membrane, with nuclear-pore complexes connecting the inside and outside of the nucleus. Small and medium-sized molecules (up to 26 nm [18]) can pass through the pores. However, bigger molecules must rely on cell division, during which the nuclear membrane temporarily disassembles, to relocate to the nucleus [19, 20]. Once in the nucleus, the plasmid is processed in the same way as gene expression of chromosomal DNA described previously: transcription takes place, the mRNA is transported to a ribosome, where it is translated into a functioning protein.

Delivering mRNA eliminates some of the steps necessary when using plasmids, as it does not require transport to the nucleus and delivering the nucleoprotein would result in the CRISPR system being already functional when entering the cell. These factors, of course, affect the time frame in which an effect can be seen, with protein being the fastest and DNA the slowest. In that sense, and since it needs to wait for cell division to enter the nucleus [19], it is fortunate that DNA is a stable molecule that can reside in the cell for a substantial period. mRNA, on the other hand, is less stable than DNA and will degrade faster, as do proteins [21]. Additionally, compared to plasmids, the production of mRNA and purified protein is complex and costly [22]. Therefore, for applications where prolonged exposure to the action of the CRISPR system is desired, plasmids are a better choice.

In this thesis work, I have delivered plasmids to cells. To assess delivery efficiency, plasmids with a green fluorescent protein (GFP) reporter were utilised, while plasmids encoding CRISPR-dCas9 complexes with an artificial transcription factor were used to achieve regulation of gene expression.

2.6 Barriers to overcome for efficient intracellular delivery

As previously stated, to regulate gene expression using plasmids, they must be delivered to the cytosol. Spontaneous cellular uptake of large molecules is limited due to membrane and enzymatic barriers in the cell [23]. All cells have a membrane separating their interior from the surrounding environment. The cell membrane consists of a lipid bilayer made of phospholipids that have a hydrophilic head group and a hydrophobic tail (see Figure 2.5a). The lipids self-organise into a bilayer to minimise contact between the hydrophobic tails and the surrounding water. Because of the tails, only small uncharged molecules (lipid soluble) can cross the bilayer to reach the cytosol, while larger and water soluble (charged or hydrophilic molecules) need other pathways to do so [24]. An example of such a pathway is endocytosis, where molecules on the outside of the cell are engulfed by the cell membrane and a vesicle is pinched off on the inside (see Figure 2.5b). The vesicle then matures into an endosome. For the molecules to affect the cell, they need to end up in the cytosol, but endosomes often fuse with, or mature into, lysosomes (the endolysosomal pathway) [25], which are cellular compartments that degrade molecules. Therefore, unless endosomal escape occurs, the molecules internalised via endocytosis do not reach the cytosol.

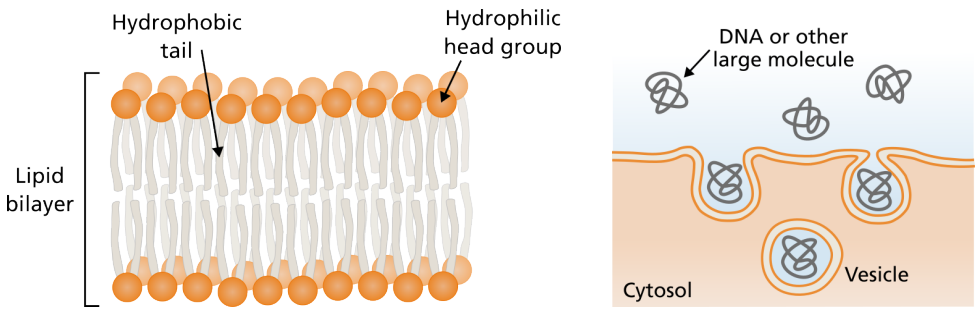

(a) Phospholipid bilayer **(b)** Endocytosis

Figure 2.5: Cell membrane composition and cellular uptake via endocytosis. **(a)** The phospholipids have a hydrophilic head group and a hydrophobic tail, which causes the molecules to self-organise into a double layer to avoid contact between the tails and surrounding water. **(b)** Large molecules are engulfed in the cell membrane, and a vesicle (endosome) is pinched off on the inside of the cell (cytosol).

To overcome these barriers, increasing the uptake efficiency, and protecting the molecules from premature degradation, intracellular delivery methods are required. There are various types of delivery methods, depending on the type of cargo that is to be delivered. In general, methods for protein delivery are not as well-established as those for nucleic acids (especially when thinking about translating it to a clinical setting, taking mRNA vaccines as an example), and are still less efficient [22]. The term used when delivering nucleic acids (DNA and RNA) to cells is transfection, which is central to this thesis. In the following sections, different types of transfection techniques will be introduced, including the method that is the main topic of this thesis.

2.7 Transfection

As no 'one size fits all' solution exists, a plethora of transfection methods are available, all suitable for different cell types and applications. These methods are generally categorised into three groups: biological, chemical, and physical. An example from each group is shown in Figure 2.6.

2.7.1 Commonly used methods and their limitations

The most common biological method by far is virus-mediated transfection, also known as transduction [26]. A virus is a small particle consisting of genetic material (which can be either RNA or DNA) surrounded by a protein capsule, called a capsid (see Figure 2.6a). After attaching to specific molecules on the cell surface, the virus can enter the cell and release its genetic material, which then replicates, new virus particles form and are subsequently released from the cell. The infectious nature of viruses can be harnessed for transfection by packaging the capsid with a nucleotide of choice and modifying the virus to prevent it from replicating inside the cell, after which it is called a viral vector. In this way, only its superb capability to transport nucleotides into the cytosol is utilised, resulting in a highly efficient transfection technique [27]. Several different virus types have been used [26], each with its own characteristics. However, there are some common drawbacks when using viruses. When delivered into cells, they can cause cytotoxicity, inflammation, and immune responses. There is also the risk of viral DNA incorporation into the cell's genome. This is a random insertion that can disrupt genes, causing harmful effects in the cells [28]. Due to these reasons, despite being a generally efficient technique, extensive research is ongoing to develop non-viral transfection methods.

The basis of chemical transfection techniques is to make complexes of negatively charged nucleic acids and positively charged chemicals that protect the nucleic acids and facilitate cellular uptake. The most used chemical is cationic lipids, which form vesicle-like structures, called liposomes, around the nucleic acids [29]. Overall, this method, called lipofection, is the most commonly used non-viral transfection technique. Other chemicals can be used, such as cationic polymers or calcium phosphate [30], but I will here focus on lipofection.

As the positively charged lipids have formed a liposome around the nucleic acid, the complex can interact with the negatively charged cell membrane and be taken up via endocytosis. Thus, endosomal entrapment is one of the fundamental issues with lipofection, causing the cargo to be degraded before reaching the cytosol. The transfection efficiency varies considerably depending on the lipid composition. While particular lipids can be used to promote endosomal escape (like positively charged lipids, which promotes fusion

with the negatively charged endosomal membrane [31]), the escape rate might still be too low [32]. Moreover, using only positively charged lipids results in a very toxic nanoparticle [33].

To achieve endosomal escape without detrimental effects on cell viability, the latest generation of lipid nanoparticles contains ionisable lipids [33]. The charge of these lipids varies with the pH. The formation of the lipid nanoparticles with incorporated nucleic acids is done in an acidic environment, where the lipids are positively charged and can interact with the negatively charged nucleic acid to form an inverted micelle around it (see Figure 2.6b). For the hydrophobic tails to avoid the surrounding water, a lipid shell forms around the inverted micelles. The suspension medium is then exchanged so that the lipid nanoparticles are neutral for non-toxic cellular delivery. Since the nanoparticles are taken up by the cell via endocytosis, they end up in endosomes. As the endosome matures into a lysosome, the interior becomes more acidic, thereby ionising the lipid nanoparticles. This results in a cationic particle that interacts with the endosomal/lysosomal membrane and escapes; however, like the liposomes, these particles also have a low escape rate [34]

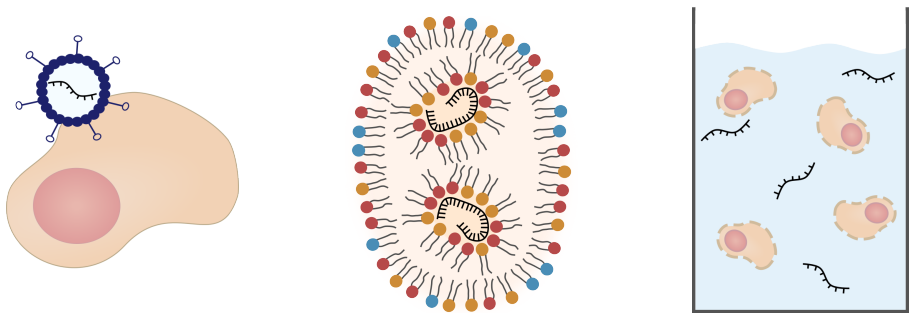

(a) Viral transduction **(b)** Lipid nanoparticle **(c)** Bulk electroporation

Figure 2.6: Three types of widely used transfection methods. **(a)** Biological method: A viral vector loaded with nucleic acids transfects a cell. **(b)** Chemical method: A lipid nanoparticle with nucleic acids inside. The different colours indicate different lipids, with red or yellow being ionisable lipids that interact with the nucleic acids and the endosomal membrane. **(c)** Physical method: Porated cells in solution with nucleic acids after application of an electric field. After poration, the nucleic acids can diffuse into the cytosol.

Physical transfection methods share the premise of using physical tools either to directly inject molecules or destabilise the cell membrane, enabling molecules to enter the cell. A growing list of these methods has emerged, including laser-assisted transfection [35], sonoporation [36], and microinjection [30], adding to the well-established and most commonly used, electroporation. I will briefly outline the working principle of the first three and then explain the mechanisms of electroporation in more detail, as it will become highly relevant in the remainder of the thesis.

In laser-assisted transfection and sonoporation, transient pores are created in the cell membrane by applying laser light or ultrasound, allowing cargo molecules to diffuse into the cell.

While the mechanisms of laser-assisted transfection are not yet well understood [35, 30], the ultrasound applied during sonoporation causes microbubbles in the surrounding medium to oscillate or rupture, which impart stresses on the cell membrane that induce the pores. A more mechanical approach is to use microinjection, which entails inserting a small needle loaded with cargo into individual cells. All these techniques manage to overcome the cell membrane barrier. However, microinjection is time-consuming due to the injection of single cells in series [35], sonoporation yields low efficiency compared to other methods [37, 38], and laser-assisted transfection has low throughput and requires expensive equipment [27, 39].

Electroporation

Electroporation was first employed in the 1980s [40] and entailed increasing the cell membrane permeability by applying an external electric field. In bulk electroporation, cells are placed in a solution of the cargo molecules and exposed to an electric field. The increased permeability of the cell membrane then allows the cargo molecules to diffuse into the cells (see Figure 2.6c).

On a molecular level, the mechanisms governing electroporation start with water molecules penetrating into the lipid bilayer (cell membrane) when exposed to an electric field. This is caused by a drive to minimise the inter-dipole interactions as well as the energy of individual dipoles in the external field [41]. The penetration of water molecules progresses, and eventually, a water channel spans across the lipid membrane, creating a hydrophobic pore. In response, the hydrophilic head groups of the phospholipids reorient and turn inwards towards the water channel to minimise the contact between the water and hydrophobic tails, creating a hydrophilic pore. This configuration is more stable and allows more molecular transport across the lipid bilayer [42].

On a membrane level, the pore size and stability, and thereby the possibility of transport across the cell membrane, is highly dependent on the strength of the electric field [43]. Depending on the field strength, the poration can be either non-detectable, reversible, or irreversible. In the range of non-detectable electroporation, there is no detectable transport of molecules. Either no pores form, or they are too small to allow any molecular transport. In a range above a certain threshold voltage, the electric field causes reversible electroporation. The formed pores are large and stable enough to allow a substantial amount of cargo molecules to diffuse into the cell, but they seal when the electric field is turned off, and hence most cells remain viable afterwards. Note, however, that the formation of pores is a statistical process and is therefore not only dependent on the threshold voltage, even though the correlation is strong. For strong fields, the pores close too slowly or not at all after turning off the electric field, leading to cell death [43, 44]. In practice, these ranges partly overlap, due to the inhomogeneity of the cells and the field across the sample, result-

ing in variations in the local electric field for each cell. This results in a distribution rather than well-defined ranges in pore formation, which induce the risk of a low cell viability when achieving efficient transfection. Additionally, electroporation can result in chemical changes in the cell membrane and its proteins, and also contribute to modifications in gene expression, thereby affecting cell function, cell viability and transport efficiency [42].

2.7.2 Utilising nanostructures for transfection

To achieve more local effects that are gentler to cells, one can utilise nanostructures for transfection. Several types of structures have been reported, but I will focus on high aspect ratio structures, which entail that the size in one direction is significantly larger than the other. The structures presented here are vertically protruding from a substrate, either configured in an array or randomly distributed on the surface, and can have various densities, thicknesses, and heights. Based on their physical properties, these high aspect nanostructures can be further grouped into solid, porous, and hollow structures [45], with examples of each introduced below. However, special attention will be given to hollow nanostructures called nanostraws, as this is what I have been working with.

Solid and porous high aspect ratio nanostructures

Solid nanostructures, or nanowires, see Figure 2.7a, have been shown to successfully deliver molecules to cells. Shalek et al. demonstrated that by depositing fluorescently labelled biomolecules, such as DNA and proteins, on solid silicon nanowire arrays before seeding cells on them, the nanowires could penetrate the cell membrane and release the biomolecules inside the cells [46]. Both a cell line and primary cells were transfected in this study, and the nanowire array was demonstrated to be minimally perturbing in both cases. In another study, several types of immune cells were instead transfected with solid nanowires [47]. Here, optimisation of nanowire density, height, and diameter was carried out to adapt to the variation in cell size and characteristics between different types of immune cells. To maintain efficient delivery and cell viability, the density needed to be decreased for smaller cells, and the height lowered for adherent cells in comparison to non-adherent cells. After optimisation, the nanowires successfully delivered fluorescently labelled biomolecules to the cells.

Nanoneedles are a type of nanostructures with a tapered or conical shape, see Figure 2.7b [48]. Chiappini et al. utilised porous nanoneedles to deliver various biomolecules into cells [49, 50]. Because the nanoneedles were made from porous silicon, they were biodegradable, with a breakdown time of under 72 hours. With these structures, they were able to measure the intracellular pH and inject quantum dots [50], as well as to regulate gene expression by

delivering silencing RNA (siRNA) (small RNA that degrades specific mRNA, preventing a protein from being produced) [49].

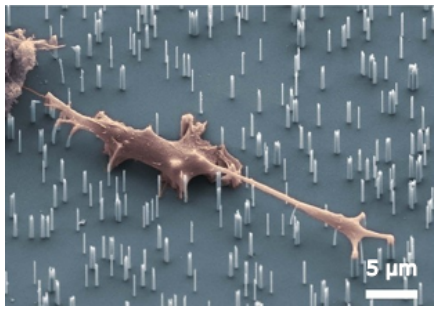

(a) Solid nanowires

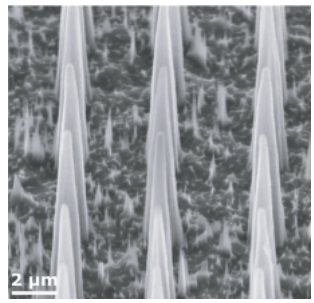

(b) Porous nanoneedles

Figure 2.7: Solid and porous nanostructures for molecular delivery to cells. **(a)** A macrophage (immune cell) cultured on a substrate with nanowires [47] (further permissions related to the image should be directed to the ACS). **(b)** An array of porous tapered nanoneedles [49]. Reproduced with permission from Springer Nature.

Although these studies showed that nanoneedles penetrate cells, a later investigation into the mechanism of cargo transfer from the nanoneedles to the interior of human stem cells revealed that the cell membrane remained intact [51]. The nanoneedles were instead found to promote endocytotic uptake of the cargo by deforming the cell membrane, which increased the delivery efficiency compared to a flat substrate. Even though a majority of the cargo was found to get trapped in endosomes, a part of the siRNA still had its intended effect, meaning that it must have either escaped before degradation or entered the cell by another mechanism than endocytosis.

Hollow high aspect ratio nanostructures

The findings described above demonstrate the need for a method where the cargo does not risk entrapment within the endolysosomal pathway, but instead is delivered directly to the cytosol. One alternative is to seed cells on a porous substrate, either flat (nanopores) or with protruding hollow nanostructures (hollow nanowires or nanostraws), with the cargo molecules kept in solution on the backside of the substrate, see Figures 2.8a and 2.8b. This system has the potential to create direct access between the backside of the substrate and the inside of the cell. Indeed, the fluid connection between the top and bottom of the substrate was demonstrated by Sköld et al., who achieved transport of DNA through a hollow nanowire substrate [52]. While this study focused solely on the fluid connection through the substrate, another study interfaced cells with the hollow nanowires and showed good viability and adherence [53]. However, to transfect cells, the hollow nanostructures also need to pierce the cell membrane. The probability of spontaneous penetration of nanostructures in the cell membrane depends on the nanostructure diameter but is generally low, and for

nanopores, it is even lower [54, 55, 56].

Physical forces have been used in combination with high aspect nanostructures to increase the probability of cell membrane permeabilisation and cargo transport. Mechanical forces -such as centrifugation or pressing - have been used to improve the penetration efficiency of solid nanowires [57, 58]. Pulsed laser light has been used for the same purpose, creating transient pores in the cell membrane over plasmonic hollow nanowires [59]. However, these methods primarily affect cell permeabilisation, not necessarily cargo transport.

To increase both membrane permeabilisation and cargo transport to the cytosol, nanostraw and nanopore substrates can be combined with the application of a pulsed electric field. This is called nanoelectroporation and is the main method used in this thesis.

2.7.3 Nanoelectroporation

As we have seen in section 2.7.1, an electric field can destabilise the cell membrane and create pores in it. In bulk electroporation, if the total potential difference across the cell membrane (resting potential plus externally applied potential) exceeds 1 V, poration can occur [60]. For bulk electroporation, reaching this value can require very strong applied electric fields. The difference between nanoelectroporation, using nanopores or nanostraws, and bulk electroporation is that, if the substrate is non-conducting, the electric field is focused to the nanoopenings (see Figure 2.8c) and will only affect the cell membrane in these areas [61]. That means that the threshold of the applied electric field can be lower while locally still achieving the same field strength and successfully opening pores in the cell membrane that interfaces the nanoopenings [62].

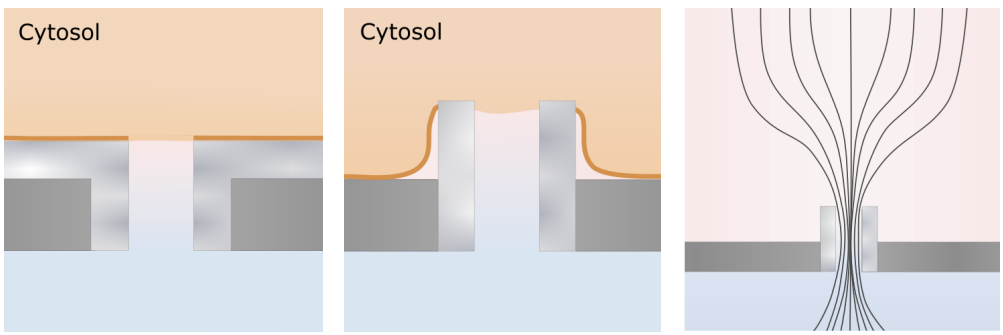

(a) Nanopore and cell **(b)** Hollow nanostructure and cell **(c)** Electric field

Figure 2.8: Concepts of nanoelectroporation. **(a)** A nanopore substrate and **(b)** a hollow nanostructure substrate with a cell seeded on top, with pores in the cell membrane (dark orange line) around the opening, creating direct access between the backside of the substrate and the cytosol (in beige). **(c)** When an electric field is applied across the substrate, the electric field lines are focused into the nanoopening if the substrate is non-conductive, allowing electroporation to occur locally when applying low voltages.

The application of an electric field not only opens pores in the cell membrane, but it can also aid cargo transport across the substrate into the cells by electrophoresis (see Figure 2.9a). Electrophoresis is the movement of charged particles in an electric field, and it can significantly improve transfection efficiency compared to the previously mentioned methods [63]. However, the behaviour of fluids in nanoscale structures diverges from that in larger structures because of the high surface-to-volume ratio. In the case of nanochannels (like the nanopores and nanostraws), depending on the material surface charge, the application of an electric field can lead to electro-osmotic flow (EOF) influencing the transport through the channels. EOF can arise owing to the formation of an electric double layer (EDL) at the nanochannel surface. Illustrations of these phenomena are shown in Figure 2.9.

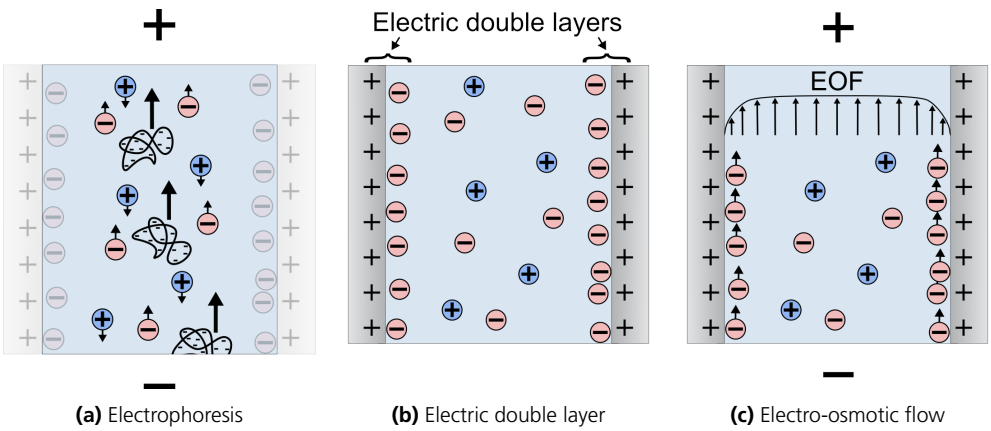

(a) Electrophoresis **(b)** Electric double layer **(c)** Electro-osmotic flow

Figure 2.9: Three mechanisms that can affect cargo transport in a nanochannel when applying an electric field. The blue particles in the solution are positive ions, and the red ones are negative ions. **(a)** When an electric field is applied along the nanochannel, it will affect charged particles in the solution, making them move towards the opposite polarity. This phenomenon is called electrophoresis. Highly charged particles, such as DNA depicted here, will be strongly affected by electrophoresis. **(b)** As the nanochannel is filled with an aqueous solution, the surface becomes charged after it chemically reacts with the solution (in this figure, positive surface charge). To screen this charge, counter ions (here negative) will accumulate close to the surface, leaving the remaining bulk fluid net neutral. The two layers of ions, the surface charge and the screening counterions, are called an electric double layer. **(c)** When an electric field is applied along the nanochannel, the ions in the electric double layer will start to move according to the field. As they do so, they drag the nearby fluid along with them, creating an electro-osmotic flow (EOF) with a flow profile as indicated. In this scenario, with a positively charged surface, the EOF and electrophoresis pull negatively charged particles in the same direction. However, in the case of a negatively charged surface, it would be the opposite situation, which may impede the electrophoretic transport of DNA to the cytosol.

An EDL is formed when a surface is submerged in an aqueous liquid, see Figure 2.9b. The surface becomes charged (due to chemical reactions with the liquid), depending on the point of zero charge of the surface (pH at which the surface has a zero net charge) and the pH of the liquid. This surface charge attracts counterions that screen the surface charge. The thickness of the EDL varies with the ionic strength of the liquid and is related to the Debye length. It can usually be up to tens of nanometres thick [64]. In nanochannels, this

can impact fluidic and molecular transport through the channel, especially if the double layers are thick enough (or the channel narrow enough) that the EDLs on opposite sides of the channel overlap [65].

When applying an electric field along the nanochannels, the ions in the EDL will move according to the field polarity, see Figure 2.9c. As the ions move, they will pull nearby fluid layers with them due to viscous forces, creating an electro-osmotic flow (EOF). Worth noting is that the electro-osmotic flow concerns the fluid's motion, not the ions'.

The molecular transport in nanochannels is affected by the particle size and charge, the ionic strength of the liquid, and the surface charge [65]. Larger particles are more likely to interact with the surface, which slows down transport. The ionic strength and surface charge affect the EDL and, thereby, the EOF, which in turn can affect the transport of particles in addition to electrophoresis. Depending on the surface charge of the channel walls and the electric field polarity (impacting the EOF direction), the electro-osmotic flow can either aid (as shown in Figure 2.9c for negative particles and positively charged surface) or impede the transport of molecules [66].

When an electric field is applied to a nanochannel connecting two reservoirs containing aqueous solutions with charged particles, both electrophoresis and diffusion (the random movement of particles within a solution) contribute to molecular transport between the reservoirs. Depending on the cargo and its location, these two mechanisms will contribute at different levels. A measure of how fast a molecule is diffusing is given by its diffusion constant D,

$$D = \frac{k_B T}{6\pi\eta r}, \tag{2.1}$$

where k_B is Boltzmann's constant, T is the temperature, η the fluid viscosity, and r the molecule radius (hydrodynamic radius in the case of a non-spherical particle). On the other hand, the electrophoretic mobility of a particle is given by

$$\mu = \frac{q}{6\pi\eta r}, \tag{2.2}$$

where q is the charge of the particle. Both D and μ are inversely proportional to r, showing that the speed of transport increases for smaller particles. However, the electrophoretic mobility also depends on the particle charge, where the transport speed increases linearly with the charge. For small molecules, diffusion is the dominant factor, while for highly charged molecules, like DNA, the primary contributor is electrophoresis.

The history of nanoelectroporation

Nanoelectroporation has been developed over the past dozen years. Some of the first mentions of using nanopores for intracellular delivery were published in 2011 [67], and 2012 for nanostraws [55, 68]. These studies did not incorporate an electric field but instead relied on spontaneous membrane piercing and subsequent diffusion of the cargo. VanDersarl et al. exposed cells to a membrane-impermeable dye via nanostraws of various diameters and found that only small diameters (100 nm) resulted in delivery, indicating that larger diameter nanostraws did not spontaneously penetrate the cell membrane [55]. The control with nanopores yielded no delivery either. Other studies used nanostraws to deliver small ions with up to 90% efficiency [69], and azidosugars (sugars with -N_3 attached) with almost 100% [70].

At this time, it was still ambiguous whether nanostraws were engulfed by the cell membrane or indeed penetrated it, which led to investigations of the cell membrane penetration mechanisms. A model for general nanowire cell penetration was put forward by Xie et al., suggesting two main mechanisms: gravitational and adherence-driven penetration [71]. Gravitational penetration entails that the cell sediments on top of the nanowire, then sinks further down and wraps around it due to the gravitational force. According to their calculations, this force was one order of magnitude lower than the force required for penetration (1-5 nN as measured by atomic force microscopy [56]). When the cell adheres to the substrate, it can generate stronger forces, even higher than required for penetration, but it is highly dependent on the nanowire geometry, as also indicated by the results of VanDersarl et al. [55]. To further elaborate on the penetration mechanisms, the effect of the cytoskeleton was studied and found to be an important factor [72]. If penetration of the cytoskeleton (along with the cell membrane) is not achieved, it could significantly shorten the time before pore closure and lead to a narrower time window for delivery [72]. However, this was refuted in the case of nanostraws when the first quantification of nanostraw penetration was presented [54], where it was observed that penetration events were stable during the experimental time frame (at least 20 minutes). They showed this by delivering Co^{2+} to GFP-expressing cells through nanostraws, quenching GFP fluorescence if delivered to the cytosol. Dark puncta appeared at each nanostraw penetration site and the penetration rate was estimated to be 7.1%. With the addition of a substrate coating with the adherence-promoting molecule fibronectin, the penetration rate increased to 12%. The cell adherence time was also found to be a contributing factor.

To increase the penetration and transfection efficiency, external forces (primarily electric fields) were coupled with the nanostraw/nanopore substrate. Nanostraw electroporation was first introduced by Xie et al. [73], who could deliver a 5 kilobase pairs (kbps) plasmid with an efficiency of 81% when using electroporation in combination with nanostraws. As a comparison, the efficiency was only 5-10% without the electric field in the same cell type

[55]. When adding the plasmid under the nanostraws substrate 10 s after electroporation, instead of it being present during electroporation, the efficiency was much lower. Moreover, the transfection efficiency decreased after reversing the polarity. Taken together, these results indicate that electrophoresis plays a significant role in plasmid transport through the nanostraws. Penetration of nanostraws was later demonstrated in another study where Stimulated Emission Depletion Microscopy (STED) was used to image the cell membrane over the nanostraw during application of an electric field [62]. The cell membrane opened over the nanostraw, allowing direct access to the cytosol (also confirmed by successful cellular extractions using nanostraws [74]). Thus, by combining the nanostraw/nanopore substrate with an electric field, both membrane permeabilisation and cargo transport to the cytosol is enhanced.

To increase the understanding of how the electric field interplays with the nanostraws and pores, both for pore formation and molecular transport, several simulations have been carried out. Focusing of the electric field to the nanostraw/nanopore has been determined [75, 76, 77, 78], with the transmembrane potential (difference in potential between the inside and outside of the cell membrane) dropping fast outside the nanochannel [79]. However, other aspects of the delivery have also been modelled, showing that the transmembrane potential achieved with nanoelectroporation exceeds the one required for pore formation at a much lower applied voltage than in bulk electroporation [77], that an increase in cell membrane tension increases delivery because more and bigger pores are formed [79], and that efficient molecular transport relies on the electric field and is maximised at an intermediate voltage [75, 79].

Various cargos, of different types and sizes, have been tested. For instance, different types of RNA have been successfully delivered: siRNA [80, 81] and microRNA that resulted in gene knockout [82], and several types of mRNA with transfection efficiencies up to 88% [82, 80, 83, 61]. Also, DNA plasmids of varying size have been transfected, ranging from about 4 kbps [79] up to 12 kbps [84]. Proteins, usually having a lower charge than nucleic acids, can be more challenging to deliver using electrophoresis-based delivery methods. Pathak et al. tested this by conjugating DNA strands to a protein and achieved an increase in transfection efficiency from 75% to 80% compared to when delivering the protein in its original form [85]. Lastly, injecting Cas9-sgRNA complexes (ribonucleoproteins), has been found to both be delivered and able to carry out its task in the cell [61, 83, 85].

Over the years, the nanostraw/nanopore substrates have been the subject of optimisation. The nanostraw length (200-3200 nm) was investigated by Schmiderer et al., who found that nanostraws shorter than 1100 nm produced transfection efficiencies exceeding 50%, while longer ones yielded progressively worse results [80]. Most of the recently published studies utilise nanostraws, but the Espinosa group has multiple reports on successful delivery using nanopore electroporation [79, 85, 81, 86]. However, a direct comparison between nanopores and nanostraws is yet to be reported. Regarding substrate pore diameter and pore density,

several diameters and densities have been used in different studies; however, no systematic comparison has been conducted to determine their effect on the transfection result. A simulation showed that higher pore density results in an overall higher transport through the substrate, supposedly up to a limit (not specified) where the substrate porosity (fraction of total pore area to membrane area) is too high and the electric field localisation disappears [79]. Experimental studies have included aspects of both porosity and pore diameter, but as other parameters were changed in the same experiment, no clear conclusions could be made for the effect of pore diameter and density alone [87, 88]. Lastly, most substrates have been based on track-etched polycarbonate (PC) or polyethylene terephthalate membranes (with or without alumina nanostraws) coated with adhesion-promoting molecules such as fibronectin or poly-L-lysine. Some attempts at making nanostraws of different materials (Au [89], SiO_x [68], conducting materials [78]) have been made, but the effect of substrate surface chemistry is still largely unexplored.

For electroporation parameters, such as pulse width, duration, and voltage, most studies include some optimisation of these parameters as they are highly dependent on cell type and application. Most have used square pulses of 100-500 µs duration instead of a constant signal to avoid heating and bubble formation. However, Pathak et al. recently tested three types of pulses: short, long, and bi-level (consisting of a higher initial voltage that is then reduced for the remainder of the pulse), and concluded that the bi-level pulses yielded the best results in terms of transfection efficiency and cell viability [85]. In the literature, the duration of electric field exposure also varies, but mostly falls within the range of 30 s to 2 min. One study showed that the optimal pulse duration depends on the applied voltage, implying there is a 'dose' effect of the electric field that should be considered [75]. The voltage is the most frequently assessed parameter and is usually kept within a range of 10-40 V. Nevertheless, as almost all studies omit to mention the distance between the electrodes, the field strength is not known, and the results can not be compared from one study to another. Another parameter, whose effect has not yet been investigated, is the choice of cargo dilution buffer.

Finally, many cell types have been tested, and with that, potential applications presented. HEK293, HeLa, and CHO have been frequently used, but other cell lines and primary cells have also been evaluated. For example, various cargos were delivered to several types of primary immune cells with high efficiency [90], five hard-to-transfect cell types were successfully transfected with mRNA [61], and primary human stem cells were found to be transfected with good viability [80]. Indeed, the nanoelectroporation method has on several occasions been demonstrated to be minimally perturbative, in regard to immediate cell viability, cell function, and gene expression [91, 80, 75, 88]. Recently, delivery of Cas9 ribonucleoproteins has been presented that resulted in successful genetic editing, which has the potential to be used in research on various diseases [85, 90, 92]. The most recently presented application demonstrates the method's capability of repeatedly injecting molecules that re-

programmed fibroblasts into induced pluripotent stem cell lines, able to differentiate [88]. These are just a few examples of the potential of this method within medical research.

Until now, no application of nanoelectroporation has been aimed towards diabetes research. In this thesis, I have addressed this by using insulin-producing cells (rat clonal β-cells) with nanostraw and nanopore electroporation. The question of how transfection efficiency and cell viability are affected by buffer conductivity, cell density, surface chemistry, and topography (nanopores versus nanostraws) will be considered in detail. Moreover, the effect of voltage is studied with a defined inter-electrode distance to enable comparison with other future studies. This optimisation will be helpful not only for the transfection of β-cells, but also to deepen the knowledge of the method in general and to continue method development. To move further towards an application in diabetes research, we modified insulin gene expression by injecting plasmids encoding a dCas9 and an artificial transcription factor. With this, we aim to take the first steps toward a new safe transfection method within the field of epigenetic editing, specifically within diabetes research.

Chapter 3

Experimental methods

3.1 Cell culture

A cell culture is the growth of cells in a controlled artificial environment. Three different types of eukaryotic cells can be grown in a laboratory: primary cells, transformed cells, and self-renewing cells. Primary cells are cells obtained directly from an animal or human, and will only live for a finite number of cell division cycles. Transformed cells, or cell lines, have genetic variations that make them immortalised; they can divide indefinitely. Lastly, self-renewing cells are cells that can differentiate into various other cell types [93]. Experiments with cells can be done either *in vitro* (greek for 'in glass'), meaning that cells are isolated and cultured long term in a laboratory setting (cell lines), or *ex vivo* (greek for 'out of the living') meaning that cells are taken out of an organism to be studied instead of being continuously cultured (primary cells).

To achieve optimal cell growth in a cell culture, the cells need to be placed in a favourable environment. To achieve this, cells are grown in a cell medium that contains all nutrients and supplements required for the cells to thrive. The cell culture is then placed in an incubator that regulates the humidity and maintains a constant temperature (37°C) and CO_2 level of 5%. The CO_2 level is used, together with a buffer in the cell culture medium, to maintain the pH level of the culture medium within the physiological range (7.2-7.4).

As the cells grow, the space and nutrients in the culture vessel are diminished, and the cells need to be split. During splitting, a fraction of the cells are removed, while new cell medium is added, to make room for the remaining cells to divide further.

In this work, we have used a rat clonal β-cell line (832/13 INS-1 rat insulinoma cells), which is an adherent cell type. Adherent cells attach to the culture vessel and grow in a monolayer,

while non-adherent cells are suspended in the culture medium. β-cells are pancreatic cells that produce insulin, a hormone that controls the level of glucose in the blood. Clonal refers to the fact that all cells originally come from one single cell, and therefore all have the same genetic material. The reason for working with these cells was that the end goal has been to optimise the method for use in diabetes research.

3.2 Nanoelectroporation

In nanoelectroporation, instead of being suspended in a solution, as in bulk electroporation, cells are seeded on a substrate with nano-openings, with the cargo molecules in solution on the other side of the substrate. As described in section 2.7.3, the cargo molecules are transported through the nanosubstrate into the cell via diffusion, EOF, and electrophoresis. This thesis deals with two main types of substrates - nanopores and protruding nanostraws, seen in the top and bottom panel of the zoom-in in Figure 3.1, respectively. The details concerning the substrates and their fabrication will be discussed in later chapters.

To achieve nanoelectroporation, the experimental setup was designed to apply electric pulses across cells and nanosubstrates. The substrates were attached to a plastic cylinder using biocompatible double-sided tape, creating a reservoir (see Figure 3.1). The cells were then seeded in these reservoirs by detaching the cells from their culturing vessel, counting

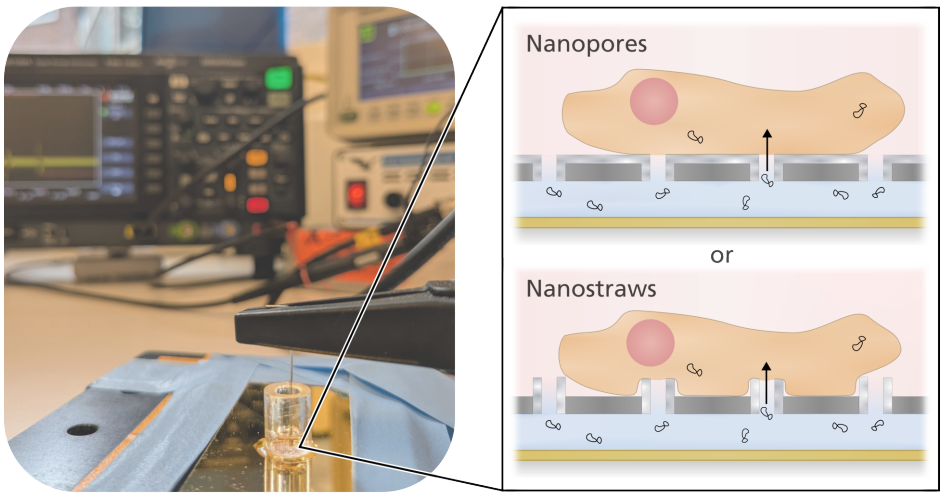

Figure 3.1: Nanoelectroporation setup. Left: Picture of the experimental setup. A polymer cylinder with the nanopore/straw substrate attached at the bottom is placed on a drop of the cargo solution on top of a gold planar electrode, and a platinum electrode (wire) is inserted into the cylinder. In the background, the signal generator, amplifier, and oscilloscope are visible. Right: Zoom-in sketch showing a cell on a nanopore (top) and nanostraw (bottom) substrate with the cargo solution and the gold-covered glass slide electrode underneath.

them, and filling the reservoir with cell medium containing the desired number of cells. The cells could either be left to sediment and adhere to the surface overnight, or the reservoirs could be gently centrifuged to spin the cells down onto the substrate. The reservoir was then placed on top of a drop of cargo solution on a planar gold electrode. The tip of the platinum wire, acting as a top electrode, was submerged in the cell medium inside the reservoir. The distance between the electrodes was kept at 0.5 mm. Both electrodes were connected to a signal generator that produced the electrical pulses and an amplifier that enhanced the signal. The electric field polarity was chosen according to the charge of the cargo molecules. For example, to pull negatively charged molecules into the cell, the positive electrode was on top. The electric field consisted of a train of square pulses instead of a steady signal to avoid heating and bubble formation. The optimal pulse width, voltage, frequency, and duration depended on the application (a combination of substrate parameters and cell type). The electrical pulses were monitored with an oscilloscope. Depending on the application, after treatment, the cells were either cultured on the nanosubstrate for later analysis, or detached and either analysed or cultured in another vessel.

3.3 Nanosubstrate fabrication and characterisation

The distinguishing feature of nanoelectroporation is the nanopore/nanostraw substrates. The starting point for fabricating nanostraws and nanopores is track-etched polycarbonate (PC) membranes, with randomly distributed pores. These polymer membranes are commercially available (it4ip, Belgium) with various pore diameters, porosities, thicknesses, materials, and surface chemistries. Depending on the nanostructure, nanostraws or nanopores, the fabrication process differs. Nanostraws protrude from the surface and require several fabrication steps, whereas nanopores are flat and only require one step, as will be described below.

3.3.1 Atomic layer deposition (ALD)

Atomic layer deposition (ALD) is the first step in making nanostraws and the only fabrication step for making nanopores. ALD is a well-established technique where monolayers of a chosen material are deposited on a surface using two vapours, called precursors, in a sequential manner [94]. The precursors TMAl ($Al_2(CH_3)_6$) and water (H_2O) were used for depositing aluminum oxide (Al_2O_3), also called alumina, on our PC membranes.

The process steps involved in creating monolayers of alumina using ALD can be seen in Figure 3.2. Each subfigure shows the cross-section of a corner of a pore in the PC membrane. The untreated PC membrane has surface hydroxyl (OH) groups (1), and the process begins with a pulse of TMAl being injected into the reaction chamber (2). The TMAl chemisorbs

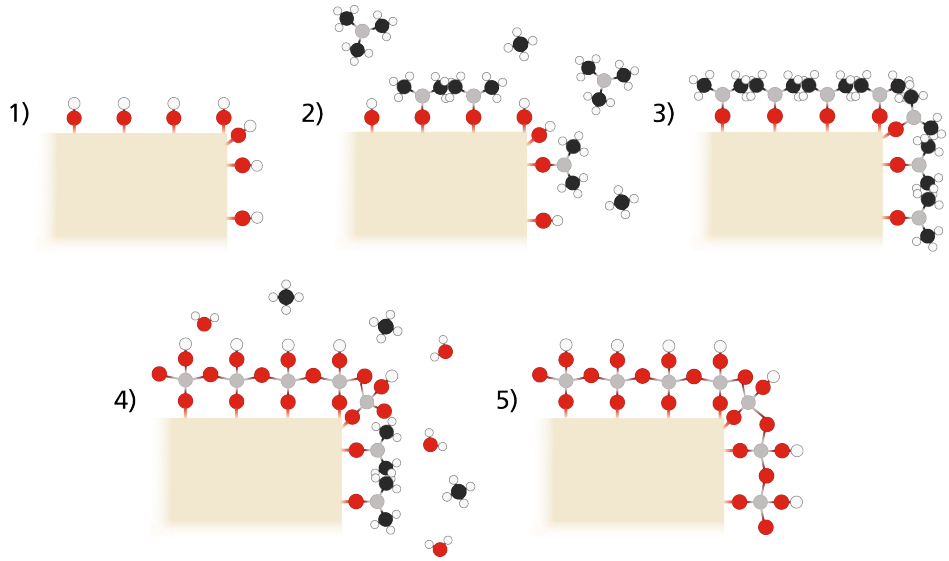

Figure 3.2: Schematics of the ALD process. The figures show a cross-section of one side of a pore in the PC membrane. The colors indicate the following species: red-oxygen, white-hydrogen, black-carbon, grey-aluminium. (1) The hydroxylated (OH) surface before processing. (2) TMAl ($Al_2(CH_3)_6$) is injected into the chamber and reacts with the hydroxyl groups on the surface, and methane (CH_4) is created in the process. The process continues until the surface is saturated (3), the chamber is then purged to remove any remaining TMAl and methane. (4) water vapour is injected into the chamber, which reacts with the surface to remove the two remaining methyl (CH_3) groups, creating methane, and resulting in the formation of a hydroxylated layer of alumina. (5) A second purge step is performed, and a new cycle can start.

(chemical bonds form between the gas molecules and the hydroxyl groups) to the surface, and methane (CH_4) is produced as a by-product. This process is self-limiting, meaning that the TMAl will adsorb until no free hydroxyl groups are left on the surface. This results in a TMAl monolayer being formed. For the process to be efficient, a temperature of 80 to 300°C is required [95]. The chamber is subsequently purged (3) to remove any remaining TMAl and methane. A pulse of water vapour is then introduced into the chamber (4). The water molecules react with the methyl groups to produce methane. Following saturation and completion of the monolayer formation, a second purge is carried out (5). A hydroxylated monolayer of alumina has now formed, and a new cycle can start. In this way, one can grow films of alumina to a precise thickness. Figure 3.2 is a schematic representation of the processes, but there is also another alternative reaction for TMAl to adsorb in (1). One TMAl can react with two hydroxyl groups to form two methane, leaving one methyl group left for further reactions. Both these reactions are most likely taking place on the surface simultaneously [95].

3.3.2 Inductively-coupled plasma reactive ion etching (ICP-RIE)

Whereas the nanopore fabrication is complete after the ALD described above, fabricating protruding nanostraws requires additional steps. Starting from the nanopore membrane, removal of the top alumina material and then some of the polymer is required. Etching is a processing technique for imprinting patterns on a surface by selectively removing material. This removal can be accomplished with liquid chemicals (wet etching) or plasma (dry etching). Dry etching techniques are highly selective (one can choose which type of material is removed) and anisotropic (it gives different etching rates in different directions), which makes it possible to create small structures and patterns with high resolution [96]. There are several available dry etching techniques, depending on the type of pattern or structure that is required.

Inductively-coupled plasma reactive ion etching (ICP-RIE) is a dry etching technique with an anisotropic etching profile. An illustration of an ICP-RIE chamber is shown in Figure 3.3. A reaction gas is injected into the vacuum chamber, and a plasma is created by an ICP source, which consists of a coil wrapped around the chamber. The ICP source generates an alternating magnetic field that oscillates at radio frequency, usually 13.56 MHz [97]. As the atoms in the gas move within the field and collide, electrons are knocked off, creating ions. Both ions and electrons are accelerated up and down in the field, but because of their larger mass, the ions move much less than the electrons. The electrons move enough to collide

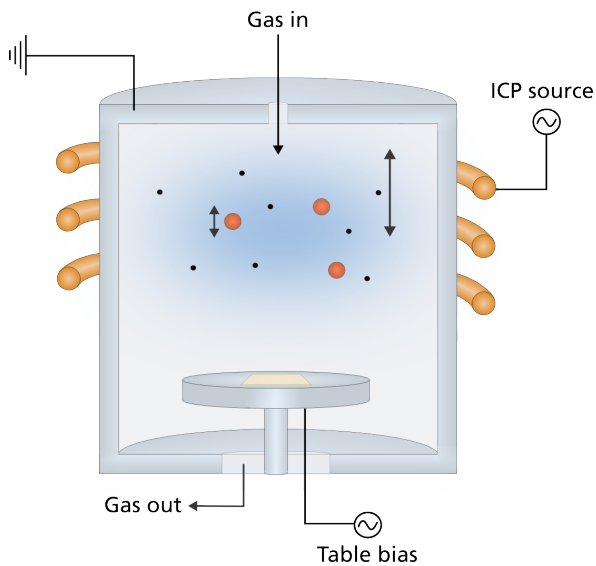

Figure 3.3: Schematic of an ICP-RIE chamber containing a plasma. The coil wrapping around the chamber, the ICP source, creates the plasma by generating an alternating magnetic field, which strips electrons from the atoms. A combination of an applied bias and a build-up of charge then accelerates ions towards the sample table, and etching occurs through both physical bombardment and chemical reactions.

with the upper wall of the chamber, as well as the sample table. As the chamber walls are grounded, those electrons are removed and are no longer part of the process. However, the sample table is isolated, and as electrons hit the table, an electric field will build up between the now slightly positive plasma and the negative sample table. Along with a separate radio frequency bias applied to the sample table, the ions are accelerated vertically towards the sample. As the ions strike the sample, they etch material vertically more than horizontally.

The main etching processes involved are physical bombardment and chemical reactions [98]. In physical bombardment, the ions that strike the substrate dislocate atoms from the surface, which are purged from the chamber. The second process involves chemically reactive species (ions, radicals, excited atoms) created in the plasma that are adsorbed onto the substrate surface, where they react with the substrate material and create volatile compounds. These compounds then desorb and are pumped out from the chamber. These two processes can be tuned by etching parameters such as gas flow, ICP voltage, table bias, and chamber pressure. The selection of gases is also crucial for the result, influencing material selectivity, anisotropy, and etch rate [97, 98].

As mentioned, in the case of nanostraws, parts of both the aluminium oxide and the PC needed be removed to yield protruding nanostraws. These two materials required different etching parameters to achieve the desired structure, and therefore, two separate etching steps were performed. For clarity, a schematic of the complete nanostraw fabrication process is shown in Figure 3.4. Using ALD, a PC membrane with pores (1) was coated with roughly 12 nm alumina (2). To make nanostraws, ICP-RIE with argon was used first to remove the horizontal layer of alumina, leaving the alumina coating inside the pores (3). The second etching step utilised sulfur hexafluoride (SF_6) and oxygen to etch the PC with higher selectivity than alumina, resulting in nanostraws extending out from the substrate (4).

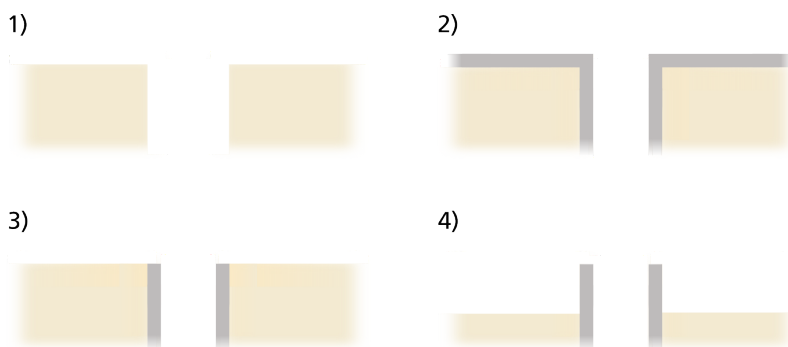

Figure 3.4: Nanosubstrate fabrication. A PC membrane (1) was coated with a layer of TMAl using ALD (2), creating nanopores. Creating nanostraws required one argon step of ICP-RIE to remove the top layer of alumina (3) and then a second step with sulfur hexafluoride (SF_6) to etch the polycarbonate (4), creating nanostraws.

3.3.3 Scanning electron microscopy

To characterise the substrates, a piece of each substrate was imaged with a scanning electron microscope (SEM). A SEM is a tool used for high-resolution imaging of nanostructures and was used to inspect and measure the dimensions of the nanostraws/nanopores. Because of the smaller wavelength of electrons compared to light, the resolution of an SEM can be as low as <1 nm, as compared to an optical microscope, which has an optimal resolution of 200 nm [99]. By scanning a focused electron beam across the sample and analysing the number of secondary- or backscattered electrons generated from each point, an image can be constructed. Secondary electrons are created when the focused electron beam knocks off electrons from the sample atoms as it scans the field of interest. They originate from near the surface, have low energy, and carry information about sample topography. Backscattered electrons, however, have high energy and are created from elastic or inelastic scattering of the electron beam on the sample. They originate from deeper in the sample. Both these types of electrons can be used for imaging.

If an insulating material is imaged in an SEM, a local build-up of electrons occurs on the sample that prevents electrons in the beam from reaching it. This can induce distortions in the image. That can be avoided by coating the sample with a few nanometres thick layer of metal, using a sputter coater. An image of nanostraws made using PC membranes with 300 nm pores and coated with 5 nm Pd:Pt can be seen in Figure 3.5.

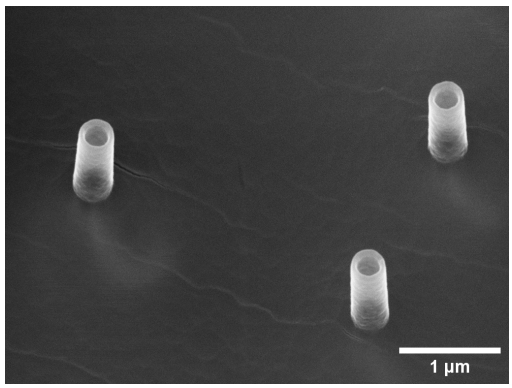

Figure 3.5: SEM image of nanostraws made using a PC substrate with 300 nm pores. The sample was coated with 5 nm Pd:Pt and the in-lens detector was used, detecting mainly secondary electrons. The stage tilt was 30°.

3.4 Analysis methods

In this work, several analysis methods were used to determine the transfection efficiency, as well as the effects of the treatment and cargo molecules on the cells.

3.4.1 Fluorescence

Several of the analysis techniques used in this thesis rely on fluorescence, which is the ability of an atom or molecule to absorb photons of a particular energy and subsequently emit photons of a lower energy. The mechanism of fluorescence begins with the absorption of a photon, leading to an electron being excited from the ground state (S_0 in Figure 3.6a) to a higher energy state (electronic energy levels, thick black lines in Figure 3.6a). The electron can lose some of its energy in non-radiative processes (wavy line), before it is de-excited to the ground state and a photon is emitted (fluorescence) at a longer wavelength than the absorbed light (Stokes shift).

In an atom, electrons have discrete and well-separated energy states, resulting in specific wavelengths being emitted when electrons transition from a higher to a lower state. Molecules, as have been used in this work, have additional degrees of freedom, vibration and rotation, that will split up the electronic energy levels (vibrational states indicated as thin black lines in Figure 3.6a). The vibrational energy states are split up further by rotational energy levels; however, these energy differences are small and not shown in Figure 3.6a. For higher electronic states, the energy difference between them decreases, leading to an overlap of the vibrational states. This results in more complex emission spectra than for atoms (which have narrow, clear peaks), see Figure 3.6b for the example of the fluorescent dye YOYO-1.

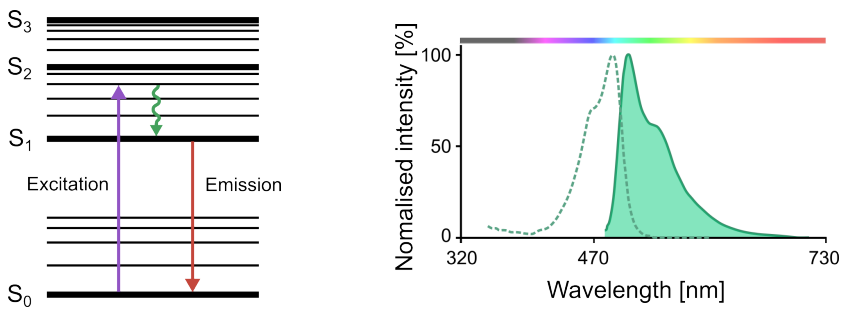

(a) Jablonski diagram **(b)** YOYO-1 excitation/emission spectra [100]

Figure 3.6: Fluorescence in a molecule. **(a)** Jablonski diagram showing electronic states as thick black lines and vibrational states as thin black lines. The purple arrow indicates excitation of an electron from the ground state S_0 to a vibrational state in the first excited state. Non-radiative relaxation occurs down to the lowest level in the first excited state (green wavy arrow), and de-excitation with photon emission is illustrated with the red arrow. Note that the emitted photon has a longer wavelength than the absorbed one; this is called the Stokes shift. **(b)** Excitation- (dashed) and emission (filled) spectra of the fluorescent molecule YOYO-1. Because of the many vibrational states present in a molecule, the excitation and emission spectra are broadened compared to those of an atom.

Fluorescent molecules

In this thesis, several fluorescent molecules and dyes have been used. They will be briefly presented below, starting with the intercalating dye YOYO-1.

An intercalating dye, such as YOYO-1, binds to double-stranded DNA, inserting itself between base pairs, and its fluorescence increases significantly when bound. The binding and unbinding of the dye to the DNA reaches equilibrium after a 2-hour incubation at about 55 °C [101]. As the dye binds, it can change the mechanical properties of the DNA [101]. However, we have seen that most of the intercalating dye unbinds from the DNA within 24 hours after transfection, and that expression of the stained plasmid is unaffected by the YOYO-1 staining 48 hours after delivery. This is due to the fact that when the plasmids are transported into the cells, their surrounding medium change to one with fewer free YOYO-1 molecules, thereby causing the equilibrium to shift, leading to YOYO-1 unbinding.

The plasmids we have used for optimisation encoded a green fluorescent protein (GFP). GFP was first discovered in jellyfish but has since been identified in several species. From these natural proteins, other variants have been engineered and are commonly used as a reporter in cell experiments.

To identify dead cells, the cell-impermeable dye DAPI was used. It increases its fluorescence intensity when bound to DNA and can thus be used to stain the cell nucleus. Since it is cell-impermeable, only dead cells with ruptured cell membranes show DAPI fluorescence.

Lastly, immunostaining was used to visualise the presence of a protein related to cell proliferation (Ki-67) in cells after nanoelectroporation. Immunostaining utilises antibodies to label target proteins. First, a primary antibody binds directly to the target protein and then secondary antibodies, labelled with a fluorophore, can bind to the primary antibody. Several secondary antibodies can bind to a single primary antibody, yielding the advantage of signal amplification in comparison to only using a labelled primary antibody. Usually, cells are fixed and permeabilised before immunostaining to prevent degradation and to open the cell membrane, respectively.

3.4.2 Fluorescence microscopy

Fluorescence microscopy was employed in this thesis to image immunostained cells. A fluorescence microscope is similar to an ordinary light microscope, but is equipped with excitation and emission filters that allow only specific wavelengths to reach the sample and detector. A schematic of the components and light path in fluorescence microscopy can be seen in Figure 3.7. A light source emits light towards a filter cube, in which it first reaches

an excitation filter that selects the wavelength that will excite the fluorescent molecule of choice. The light then encounters a dichroic mirror that reflects it towards the sample. A dichroic mirror has a cut-off wavelength, below which light is reflected, while light with a longer wavelength is transmitted, or vice versa. The excitation light leaves the filter cube and is focused onto the sample by an objective. The fluorophores present in the sample absorb the excitation light and emit light at a longer wavelength, as previously described. The fluorescence emitted towards the detector will first be transmitted through the dichroic mirror and then reach the emission filter. The emission filter blocks unwanted light, while it allows the fluorescence from the fluorophore to pass. Depending on the chosen filter cube (excitation filter, dichroic mirror, and emission filter), and thereby which wavelengths that are selected, different fluorescent molecules can be visualised.

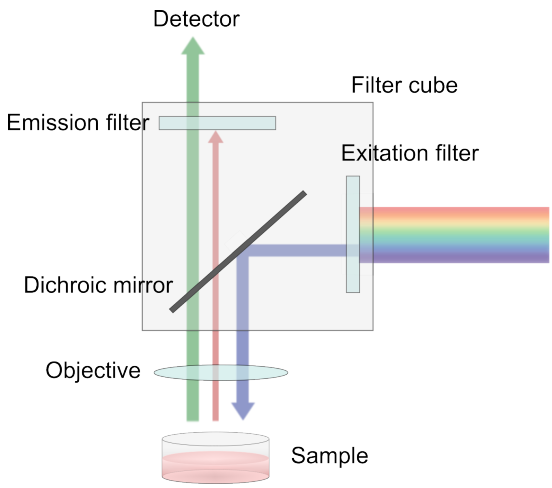

Figure 3.7: Schematic of a fluorescence microscope. A light source emits light, which passes through a filter cube that selects the excitation wavelength. A dichroic mirror, deflecting wavelengths shorter than the cut-off wavelength while transmitting longer wavelengths, redirects the light towards the objective and sample. After excitation, the fluorescently labelled cells in the sample emit light at a longer wavelength, which passes through the mirror and emission filter (while other wavelengths are blocked) to finally reach the detector.

3.4.3 Flow cytometry for immediate analysis of transfection efficiency

Flow cytometry has been the most frequently used analysis method in this work as it is operationally simple and time-efficient. It is a technique for counting and analysing the properties of a set of cells in suspension by scattering or fluorescence. I have used it to evaluate transfection efficiency, cell viability, and cell count after transfection. A schematic of a flow cytometry machine can be seen in Figure 3.8.

In flow cytometry, a cell suspension containing differently labelled cells is loaded into the machine, where the cells are focused into a single line by a flowing sheath fluid and moves

through a laser beam, one at a time. The sample flows within the sheath fluid, but the two fluids do not mix (due to laminar flow), a phenomenon called hydrodynamic focusing. As a cell moves through the laser beam, it scatters the incoming light. Light deflected mainly by the cell membrane is detected along the same axis as the laser, called forward scatter (FSC) light, which provides information about the cell size. Light scattered at larger angles is usually detected at a 90° angle from the beam and is called side scatter (SSC) light. This light is scattered mostly by cell constituents and thus carries information about the cell's granularity [102].

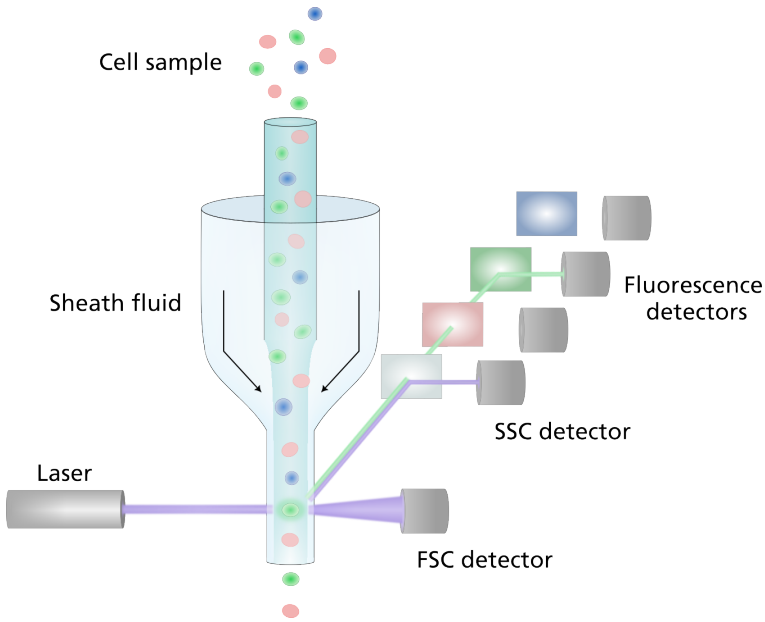

Figure 3.8: Schematic of a flow cytometry setup. The cells are loaded from the top and directed into a flow of single cells by a sheath fluid. The single cells flow through a laser and scatter the light in a forward direction, detected by the forward scatter (FSC) detector, which gives information about the cell size. Cells also scatter light at an angle compared to the incoming beam direction, detected by the side scatter (SSC) detector, which provides information about cell granularity. If the cells are fluorescently labelled, the emitted fluorescence will encounter dichroic mirrors and be directed into the right detector.

Flow cytometry can also assess the fluorescence of cells that are stained with different fluorescent dyes (fluorophores). An example is shown in Figure 3.8, where unlabelled cells are pink, and cells stained green and blue are shown in their respective colours. When a labelled cell moves through the laser, the incoming light excites the fluorophore, which then emits light of a different wavelength. The fluorescence light is collected in the same direction as the SSC light. However, the wavelengths are separated by dichroic mirrors and the emission light that goes through the first mirror (where the side scatter light is redirected to its detector) is redirected into the right detector/channel by a set of other dichroic mirrors. Several fluorophores can be used in the same sample, as long as their spectra do

not largely overlap. Due to partial spectral overlap between fluorophores, compensation between channels might also be necessary to avoid signal spillover from one channel to another.

Gating

When acquiring flow cytometry data, subsets of cells can be selected and subsequently analysed. This selection is called gating and can be done in several steps, until only the target cell population remains in the analysis. In this way, data from different populations in the sample can be separated and analysed individually. An example of a gating for clonal β-cells transfected with YOYO-1-stained plasmids is shown in Figure 3.9.

Starting from the top left (panel a), the entire measured population is visible in this panel. Ideally, each dot corresponds to the signal of one cell. Both the x and y-axis show FSC, but the difference between them is that the x-axis shows the area of the signal (indicated with -A), and the y-axis the height (denoted with -H). As a cell moves through the laser, the measured intensity signal will be a curve with a height and width, see the left side of the inset in (a). When single cells move through the laser, the area of the curve is proportional to the height, and these cells should lie on a straight line in the data plot, selected within the green box. The dots deviating from the straight line, following a different slope, are aggregations of cells (mostly doublets). Compared to single cells, these will have an intensity curve with a larger area relative to their height, as shown in the right side of the inset in (a). That is because they take longer to pass through the laser, and the signal is therefore broader, while maintaining the same height as for the single cell signal. These aggregates are excluded from the analysis since one count represents the average of several cells rather than a single cell, which would increase the risk of acquiring false positives. From panel (a), only the counts within the green box are carried over to the next panel for further analysis.

In Figure 3.9b, the signal included in the green box in (a) is displayed in terms of FSC-A on the x-axis and SSC-A on the y-axis. Debris, objects in the sample solution that are large enough to be detected, but too small to be cells, can be seen in the lower left corner in (b). Since only whole cells are of interest here, these counts are excluded from the analysis by the blue gate.

The remaining cells after excluding aggregates and debris are displayed in Figure 3.9c, where the next step is to exclude dead cells from the analysis. For this, DAPI (which fluorescence is displayed on the y-axis of (c)) is mixed into the sample solution, and DAPI-positive cells (i.e. dead cells) are counted in the red box in panel (c). The cell counts in the turquoise box in (c) correspond to the single, live cells that should be evaluated for the presence of the target fluorophore and cell count, in this case, the green fluorescence of YOYO-1 labelled plasmids. That signal is displayed in Figure 3.9d with FSC-A on the x-axis and YOYO-1

fluorescence on the y-axis. To set the gating for this population at a correct level in terms of fluorescence, the green box is adjusted according to a control sample without fluorescently labelled plasmids. Cells showing green fluorescence, in this case, cells successfully injected with the plasmid, are selected within the green box in (d).

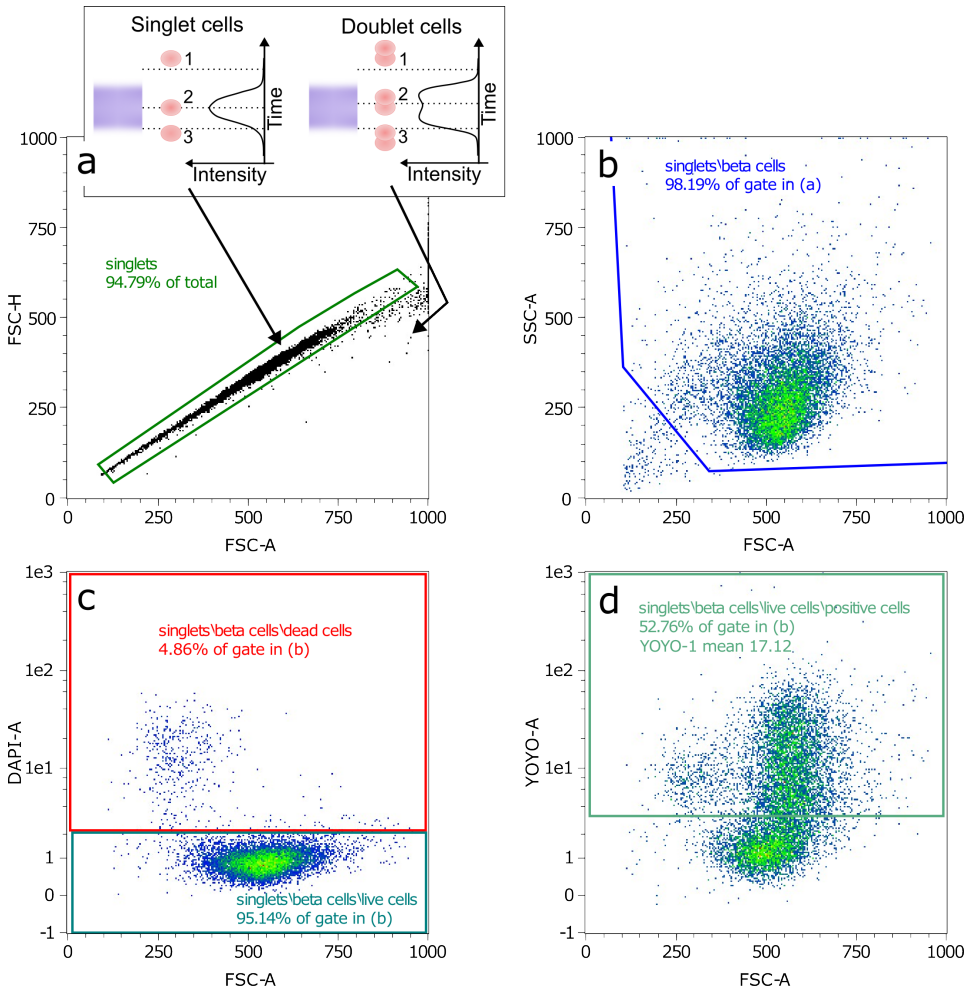

Figure 3.9: An example of a gating strategy used in this thesis work. All x-axes represent forward scatter signal area (FSC-A), and the y-axes are explained in parentheses for each panel. In (a) (forward scatter signal height (FSC-H)), all measured particles are displayed. The singlet cells are chosen with the green box for further analysis. The inset shows the different appearances between signals originating from single and doublet cells as they move through the laser (purple). Three time points for the cell and aggregate, respectively, are indicated as 1, 2, and 3 with corresponding dashed lines. Both signals have equal height, but since the doublet cells have a wider signal, they will lie on a different slope, outside the green box, in the FSC-H vs FSC-A plot. In (b) (side scatter (SSC)), the debris is removed, and only whole cells are displayed in (c) (DAPI fluorescence), where dead cells are excluded based on whether they are positive for the cell impermeable dye DAPI. Finally, in (d) (YOYO-1 fluorescence), the number of cells positive for the injected green plasmid is assessed with the green box. The lower level of this box is based on a control sample where no plasmids were injected.

3.4.4 Phase holographic microscopy

Phase holographic microscopy is a digital microscopy method used to image cells without the use of fluorescent labels and to obtain three-dimensional information. Moreover, these microscopes have motorised stages and can be placed inside an incubator, meaning one can acquire time-lapses of multiple locations on the cell culture substrate, all while the cells are kept in optimal conditions. In my work, I have used phase holographic microscopy to image cells on various substrates to study the effect of surface chemistry, as well as after transfection to investigate how the cells were affected by the treatment.

The basic principles of this technique stem from how holograms are made. In contrast to ordinary photography, where intensity and wavelength are used to create an image, a holograph is made by utilising the light's phase. A sketch of the microscope setup (the same as for creating any hologram, just exchange the cell sample with any other object of interest) can be seen in Figure 3.10.

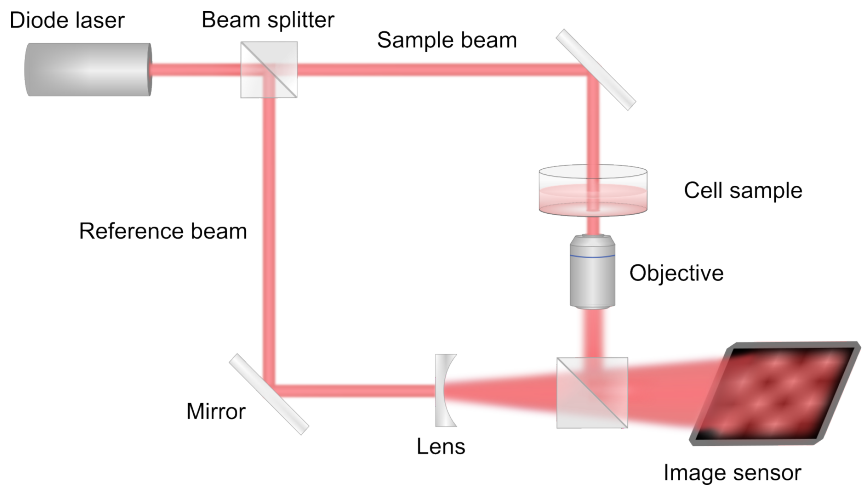

Figure 3.10: Sketch of a phase holographic microscopy setup. The laser beam is split into one reference beam and one sample beam. The sample beam passes through the sample, where the phase of the light is affected, while the reference beam passes unperturbed to the image sensor. The two beams are then joined before the image sensor to create an interference pattern. With the help of software, it is possible to extract 3D information about the sample.

The beam from a diode laser is divided by a beam splitter into two identical beams, the sample beam and the reference beam. Since information about the phase is critical, the coherent light (meaning all photons have the same wavelength and phase) of a laser is required. The reference beam goes unperturbed through the system and then illuminates the image sensor after being reunited with the sample beam. The sample beam instead goes through the sample before reaching the image sensor. The optically denser cells will affect the phase of the light, and the two beams will create an interference pattern when

they coincide again. This interference pattern is recorded on the image sensor and with the provided software, the recorded pattern will be turned into an image of the cells. And just as in any hologram, 3D information is contained within the interference pattern, and the height of the cells can be visualised.

3.4.5 Quantitative polymerase chain reaction (qPCR)

Quantitative polymerase chain reaction (qPCR) is a method for detecting specific RNA or DNA sequences in a sample. It has been used in this thesis to analyse the expression of insulin mRNA after injection of the dCas9-repressor plasmid complexes in Paper III.

In qPCR, a specific DNA sequence is amplified while its amount is analysed in real time. When assessing gene expression, RNA is extracted from the cells and converted into complementary DNA (cDNA) before qPCR can be performed. This conversion is called reverse transcription. It starts with that short DNA sequences, called primers, anneal to the mRNA and act as starting points for DNA synthesis by the enzyme reverse transcriptase. The primers are designed to match a short sequence on the mRNA that flanks the target sequence. As the reverse transcription is finalised and all mRNAs are hybridised with a cDNA, the reverse transcriptase is deactivated with heat to ensure a 1:1 ratio of cDNA to mRNA.

qPCR entails a cyclic exponential amplification of the cDNA. A schematic of the process for the first three cycles is displayed in Figure 3.11. The first cycle starts with the addition of the necessary reagents and heating the solution to separate the mRNA from the cDNA. It is then cooled down again to allow primers and probes to anneal to their corresponding sequences. The primers, which act as the starting points for DNA synthesis, are designed to anneal outside of the target sequence on the cDNA, while the probe (containing a fluorophore and quencher) anneals on it. Complementary nucleotides are connected by a DNA polymerase (enzyme), which, when it reaches the probe, degrades it as it continues to synthesise DNA. As the probe is degraded, the fluorophore is released from the quencher and starts to fluoresce upon excitation. The probe matches a specific sequence on the DNA, which ensures that only one fluorophore is released per new copy of DNA.

There are two versions of the primers, one forward and one reverse, each matching a sequence on one of the long DNA strands - the original cDNA strand and the product of the first cycle (blue and green in 'Second cycle' in Figure 3.11). Together, these two primers flank the target sequence and result in the synthesis of short strands, which include only the target sequence and the two flanking primer sites. These short strands are then amplified exponentially in subsequent cycles, with one fluorophore released per newly synthesised DNA copy, resulting in the fluorescence exponentially increasing.

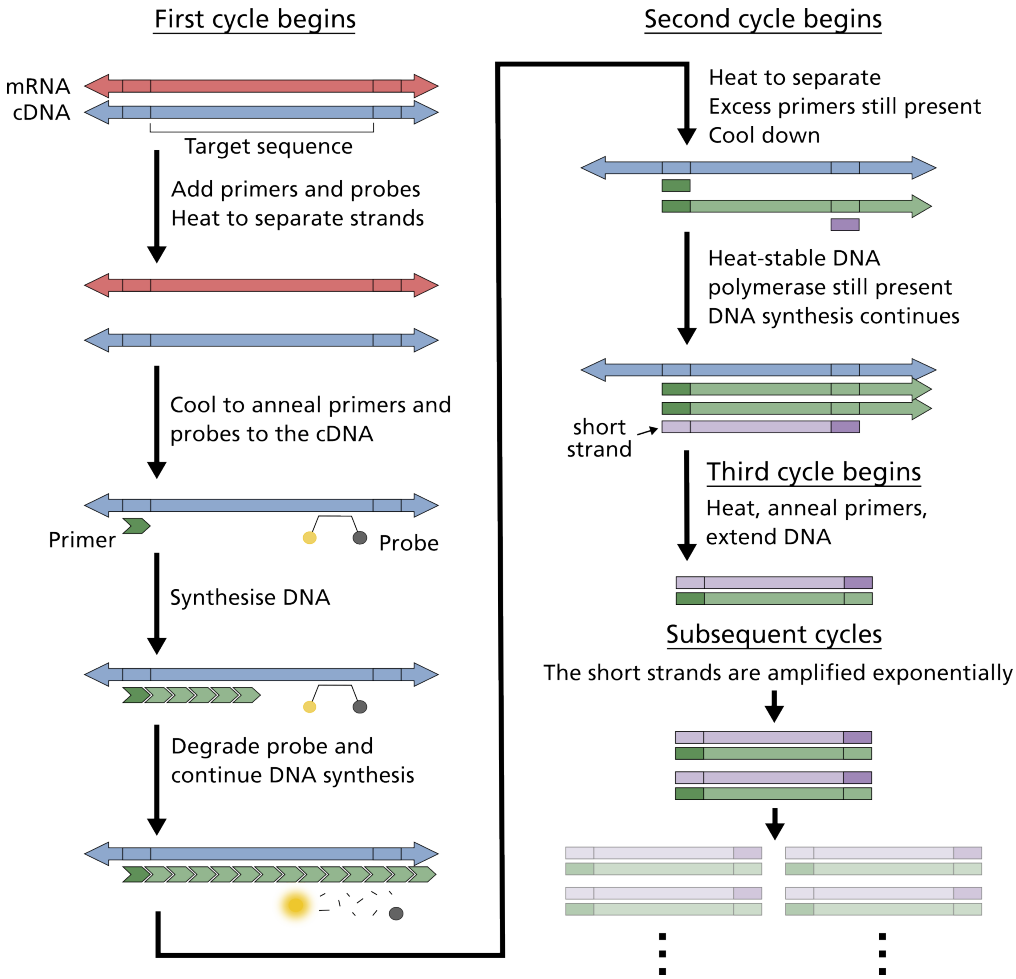

Figure 3.11: The first cycles in the qPCR amplification process. The first cycle starts with that primers and probes are added, and the sample is heated to separate the mRNA and cDNA strands. It is then cooled down to allow for the primers and probes to anneal to the target sequence. DNA polymerase (not shown) initiates DNA synthesis from the primer, and as it reaches the probe, the probe is degraded. The fluorophore is then released from the quencher and starts to fluoresce. In the second cycle, the two different primers result in short strands being produced, which are exponentially amplified in subsequent cycles.

The C_T value is the number of cycles required to reach a certain fluorescence threshold level and is inversely proportional to the initial number of mRNA molecules in the sample. For example, a low amount of mRNA in the sample requires more amplification cycles before reaching the threshold, and thus, the C_T value is high. The threshold is determined by the software, based on the fluorescence background level of all samples for a particular gene. To account for differences between samples (for example, the amount of extracted RNA), a control gene can be used to normalise the result of the target gene. These control genes are commonly involved in basic cellular functions and is selected based on the fact that

its expression is stable across different samples. For reliable comparison between sample groups, some processing of the C_T values is required, more than just normalising to the control gene. The C_T value of the control gene is subtracted from the C_T value of the target gene, giving the ΔC_T. Then, the ΔC_T of the control sample is subtracted from the ΔC_T of the test sample. The result is called the $\Delta\Delta C_T$ value and gives the relative expression level of the target gene compared to both the control gene and control sample.

Chapter 4

Results - Optimisation of nanoelectroporation transfection parameters

As described in the background chapter, several aspects of nanoelectroporation still need investigation, which we have addressed in papers I and II. In addition, since nanoelectroporation has not yet been used with rat clonal β-cells, it has been crucial to optimise the method for these cells and determine how they react to the treatment. While the first paper mainly focuses on electroporation parameters, the second paper instead handles factors related to the nanopore/nanostraw substrate. Note that the electrode distance, often lacking in literature, is set to 0.5 mm in all experiments in this thesis.

4.1 Means to assess transfection efficiency

To assess the transfection efficiency, the cargo molecules in these two papers were two types of GFP-expressing plasmids, pMAX (3.5 kbps) and eGFP (6.1 kbps). These plasmids were either injected as they were or stained with the intercalating fluorescent dye YOYO-1, as illustrated in Figure 4.1. When the plasmids were transfected as they were, they needed 48 hours to be expressed by the cell before GFP fluorescence could be assessed. On the other hand, the YOYO-1 staining procedure allowed for assessment of transfection efficiency immediately after transfection, as the DNA was already fluorescent. In both cases, the cell fluorescence was assessed using flow cytometry after staining dead cells with the cell-impermeable dye DAPI. When YOYO-1 have been used in this thesis, the DNA have been stained at a molecular ratio of one YOYO-1 molecule per 250 base pairs.

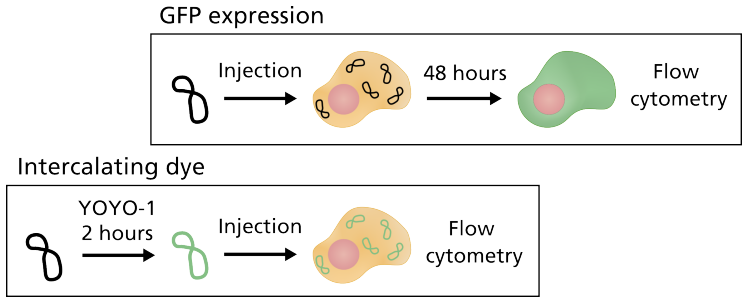

Figure 4.1: Overview of the two methods for evaluating the transfection efficiency when injecting GFP-expressing plasmids. The first method assessed the GFP expression of the plasmids after a 48-hour waiting period. Using the second method, plasmids were stained with the intercalating dye YOYO-1, and transfection was evaluated immediately after delivery.

4.2 Optimising electroporation parameters - Results of Paper I

This paper aimed to investigate the effects of electroporation parameters such as voltage, cell density, and cargo buffer conductivity, on transfection efficiency and cell viability of rat clonal β-cells. For these experiments, the pMAX plasmid was stained with YOYO-1 before injection, and the samples were analysed immediately after nanostraw electroporation using flow cytometry. As a final point, injection using nanostraws and nanopores was compared, both in terms of immediate transfection (internalised YOYO-1-stained plasmid) and after 48 hours (GFP-expression).

First, the effect of applied voltage was examined by varying it between 14 V and 36 V. The results can be seen in Figure 4.2. Up to 33 V, the transfection efficiency increased with

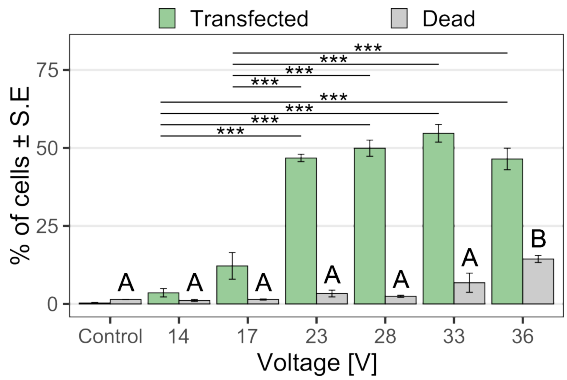

Figure 4.2: Optimisation of voltage during nanostraw electroporation on β-cells. Transfection efficiency (green) and cell death (grey). Significantly different groups, calculated with ANOVA and Tukey Post Hoc test, are indicated by horizontal lines and stars (***: $p<0.001$) for the transfection efficiency, and by capital letters for cell viability, with $p<0.05$. (n = 3, error bars indicate standard error)

higher applied voltage. When the voltage was increased further, the transfection efficiency decreased slightly, and cell death was significantly higher. Using 28 V resulted in the next-to-highest transfection efficiency while maintaining the cell viability as high as possible. We therefore used 28 V in the remainder of Paper I and in Paper II.

Next, the question of how cell density affects transfection efficiency was addressed. A thought within the field had been that uncovered nanostraws could pose a problem during nanoelectroporation by lowering the resistance of the porous substrate, thereby decreasing cargo delivery [103]. One way to minimise the number of uncovered nanostraws is to maximise cell density. To test this, we varied the cell density in our samples, from very sparse to more than a completely covered surface, as seen in Figure 4.3. Going from the highest

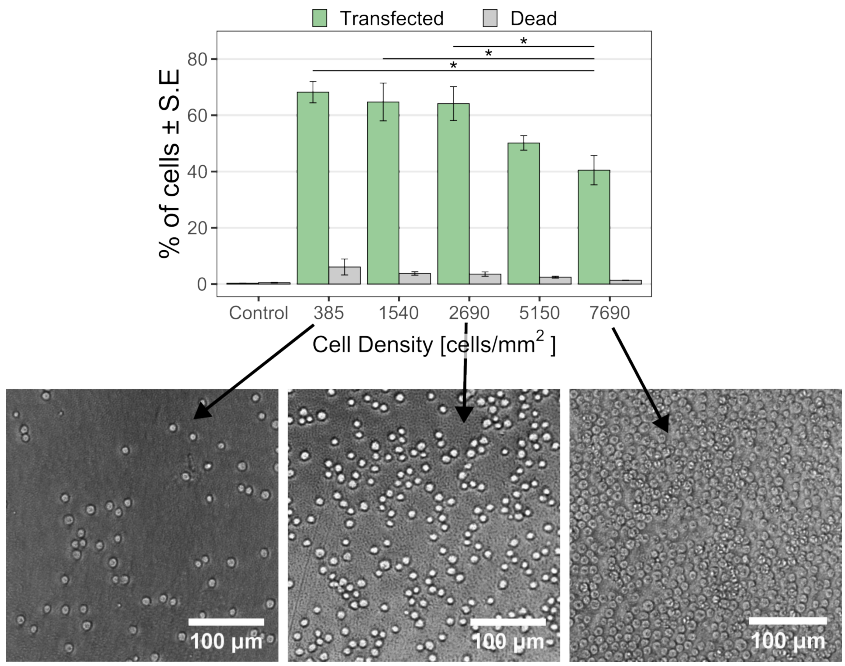

Figure 4.3: Optimisation of clonal β-cell density on the nanostraw substrate during nanoelectroporation. The top panel show the transfection efficiency (green) and the cell death (grey) after transfection with YOYO-1-stained plasmids. Below are microscopy images of three of the tested densities, as indicated by arrows. (n = 3, error bars indicate standard error. Statistics: ANOVA and Tukey Post Hoc test, *: $p<0.05$).

cell density to the lowest, the transfection efficiency first increased and then reached a plateau for densities below 2690 cells/mm^2. We explained the lower transfection efficiency at high cell densities by the fact that at higher densities, cells stack on top of each other and are therefore not all in contact with the substrate, which means many cells cannot receive any cargo. That indicated that as long as cells were in contact with the substrate, the electrophoretic force exerted on the cargo was not dependent on the number of uncovered nanostraws. From here on, the remainder of the experiments in this thesis were

conducted using a cell density of 2690 cells/mm^2 to balance scalability with achieving a high percentage of transfected cells.

The buffer used to dilute the cargo molecules had not previously received much attention, although several different buffers have been used in previous studies. We tested the effect of buffer conductivity on transfection efficiency and viability, with conductivities ranging from 0.001 mS/cm for MQ water to 78 mS/cm for 10x concentrated DPBS. The results are displayed in Figure 4.4.

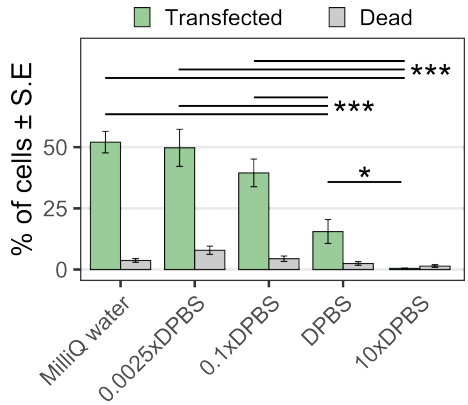

Figure 4.4: Optimisation of the plasmid buffer conductivity. Cells were injected with YOYO-1-stained plasmids and analysed directly after transfection. Transfection efficiency is shown as green bars and cell death as grey bars. ($n \leq 3$, error bars indicate standard error. Statistics: ANOVA and Tukey Post Hoc test with ***: $p<0.001$, *:$p<0.05$).

Although the cell viability was unaffected, the transfection efficiency decreased with increasing buffer conductivity. To explain this, we turned to simulations of the voltage drop across the nanostraw substrate. The higher the voltage drop across the substrate, the stronger the electrophoretic force exerted on the plasmids is. The simulation results showed that the highest voltage drop was achieved with MilliQ water, while the lowest was with 10x DPBS, which conformed to the experimental results.

The last part of Paper I involved a first comparison between nanopores and nanostraws. The results can be seen in Figure 4.5. There was no significant difference in immediate transfection efficiency identified; however, a significantly larger fraction of cells expressed GFP 48 hours after transfection with nanopores compared to with nanostraws (Figure 4.5a). When looking at the mean intensities in Figure 4.5b, nanostraws gave a higher intensity at both time points, indicating that more plasmids were injected per cell. The observations that a similar percentage of cells were transfected with both substrates, but nanostraws injected more plasmids per cell, were contradictory to the lower cell percentage expressing GFP after 48 hours. Because of the lower cell count 48 hours after transfection using nanostraws compared to nanopores (Figure 4.5c), we speculated that this discrepancy could have two explanations: either more cells died after transfection with nanostraws, or the cells prolif-

erated less, inhibiting the translocation of the plasmids to the nucleus and thus preventing expression [19]. At this point, we could not determine the cause of the discrepancy; however, this matter was further investigated in Paper II.

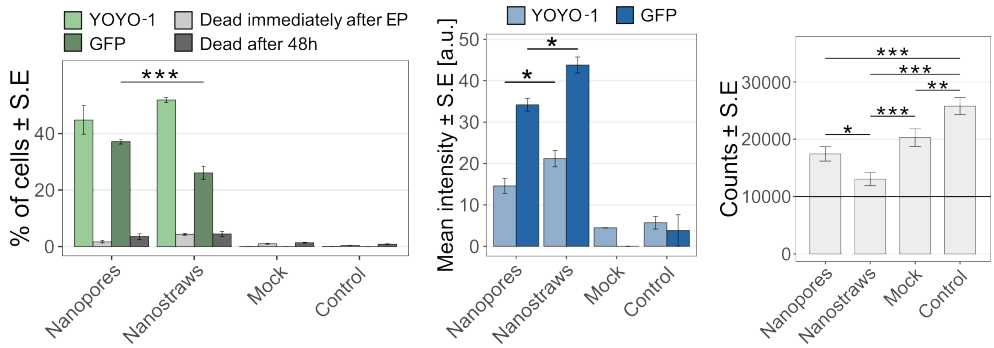

(a) Transfection efficiency and cell viability **(b)** Mean fluorescent intensity **(c)** Cell count after 48 hours

Figure 4.5: Comparison of nanopore and nanostraw substrates for nanoelectroporation. Part of the cells were analysed directly after transfection and some were cultured and assessed 48 hours later for GFP expression. **(a)** Transfection efficiency, both immediately after transfection (light green) and 48 hours later (dark green). The cell death immediately after, and 48 hours after, transfection is shown in light and dark grey, respectively. **(b)** The mean fluorescence intensity of transfected cells, YOYO-1 in light blue and GFP in dark blue. **(c)** The cell count 48 hours after transfection when 8000 cells were seeded of each sample after transfection (indicated with black horizontal line). ($n \leq 3$, error bars indicate standard error. Statistics: in (a) and (b) t-tests were used, and in (c) ANOVA and Tukey Post Hoc test: ***$p < 0.001$, **$p < 0.01$, *$p < 0.05$).

4.3 Optimisation of substrate parameters - Results of Paper II

In this paper, we explored the effect of nanopore/nanostraw substrate parameters, such as porosity, pore diameter, surface chemistry, and topography. Nanopores were used to first evaluate the influence of porosity, diameter, and surface chemistry by transfecting the pMAX plasmid stained with YOYO-1. Subsequently, nanopores and two types of nanostraws were compared in terms of transfection efficiency, both immediately and 48 hours after transfection. These experiments were conducted with the larger eGFP plasmid. The discrepancy found in Paper I, between the percentage of cells transfected immediately and the fraction of cells that expressed GFP after 48 hours, was thoroughly investigated. To do this, five types of nanosubstrates were fabricated, as shown in Figure 4.6.

First, the effect of porosity, pore diameter, and surface chemistry on nanopore electroporation was evaluated. For the porosity experiments, three different porosities (with pores covering 0.6%, 0.2%, and 0.06% of the substrate surface area) were tested and the results showed that higher porosity yielded higher transfection efficiency (Figure 4.7a). A possible reason for this was that, for the lower porosities, the distance between nanopores was large enough for cells to interface with too few nanopores to receive a detectable amount of plas-

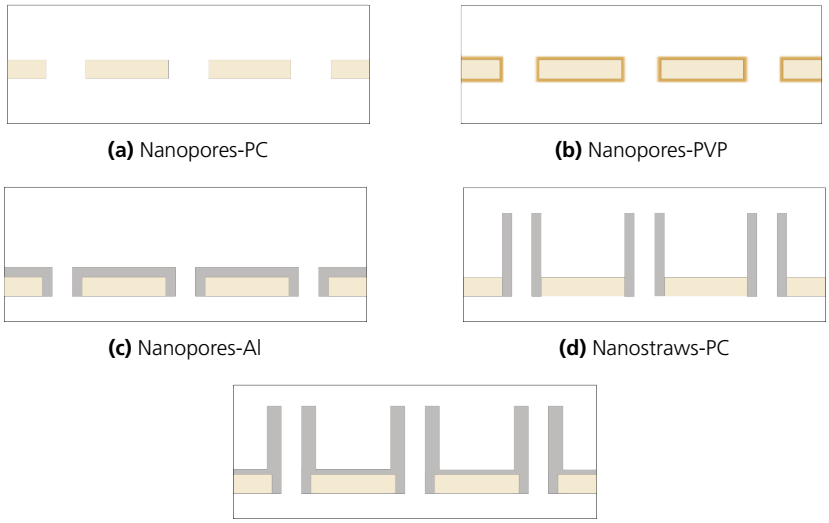

Figure 4.6: Schematics of the five different types of substrates used for the experiments in Paper II, with PC in beige, polyvinylpyrrolidon (PVP) in orange, and alumina in grey. **(a)** Nanopores with a PC-surface (Nanopores-PC), used as purchased. **(b)** Nanopores with a PVP coating (Nanopores-PVP), used as purchased. **(c)** Alumina-coated nanopores (Nanopores-Al), **(d)** nanostraws with PC surface between the nanostraws (Nanostraws-PC), and **(e)** nanostraws with alumina surface between the nanostraws.

mid. Next, a comparison of two nanopore diameters was conducted, which showed that using 200 nm nanopores led to a higher amount of transfected cells, as well as higher cell viability compared to when using 300 nm nanopores (Figure 4.7b). Lastly, three substrate surface chemistries were compared: PC, PVP, and alumina (a, b, and c in Figure 4.6). The highest transfection efficiency, by far, was observed for the alumina surface (see Figure 4.7c). From these results, we found that the best choice for nanopore electroporation was nanopores-Al with 200 nm diameter pores and 0.6% porosity.

Since cell-surface interactions have been shown to play a significant role in achieving successful nanoelectroporation, we explored whether this contributed to the substantial difference in transfection efficiency between the three surface chemistries discussed above. Cells were imaged on the three substrates for 24 hours using phase holographic microscopy. Cells on the various substrates after 20 hours of imaging can be seen in Figure 4.8. The cells cultured on PVP and PC substrates clumped together and formed aggregates that grew vertically, while cells on an alumina coated substrate spread out on the surface. The tendency to form aggregates was already visible after 5 hours, and even after 1 hour, the cells started to group on the PVP and PC. Since a good cell-substrate seal is required for efficient nanoelectroporation transfection, the poor transfection efficiency observed for PVP and PC may, at least partly, be explained by poor cell adhesion.

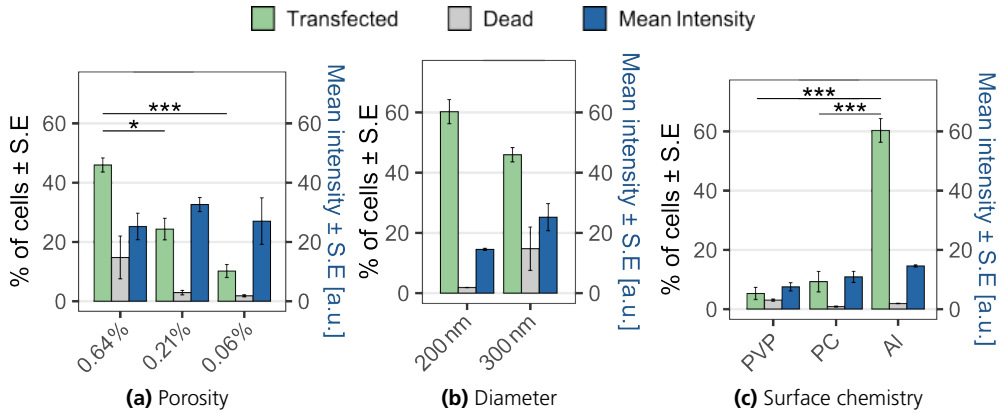

Figure 4.7: Optimisation of substrate parameters. The effect of **(a)** substrate porosity, **(b)** pore diameter, and **(c)** surface chemistry on transfection efficiency (green), cell death (grey), and mean fluorescence intensity of transfected cells (blue). Cells were injected with YOYO-1-stained plasmids and analysed directly after transfection. (n=3, the statistics were calculated with ANOVA and Tukey Post Hoc test with: ***: p<0.001, *: p<0.05).

Subsequently, the combined effect of surface chemistry and topography was studied by comparing nanopores-Al, nanostraws-PC, and nanostraws-Al (see panels c, d, and e in Figure 4.6). To assess the transfection efficiency, the eGFP plasmid was stained with YOYO-1 before delivery. Part of the cells were analysed immediately using flow cytometry, while 8000 cells were seeded to be analysed 48 hours later. The immediate transfection efficiency was higher for nanostraws-PC compared to nanopores-Al (Figure 4.9). Using nanostraws-

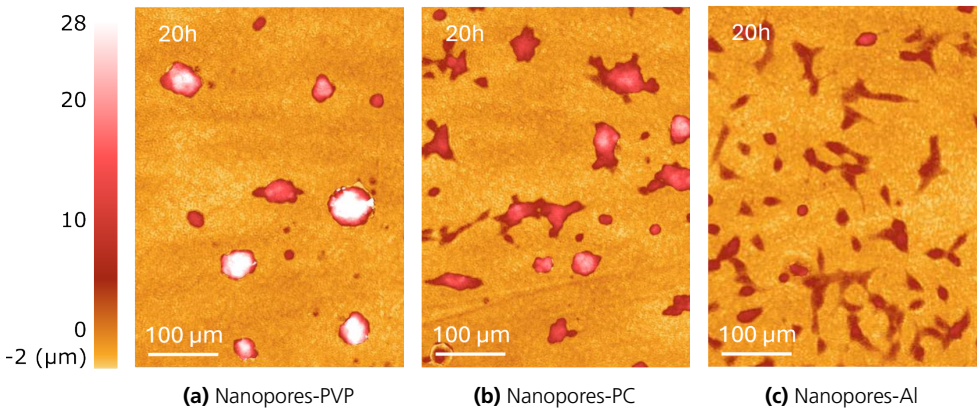

Figure 4.8: Phaseholographic images of the cells cultured on **(a)** nanopores-PVP, **(b)** nanopores-PC, and **(c)** nanopores-Al, respectively. The cells were seeded on the substrates in equal concentration and cultured for 24 hours. The images shown here are taken 20 hours after seeding.

Al provided an even higher fraction of transfected cells and we concluded that the alumina surface between the nanostraws was, in fact, the reason why nanostraws-Al outperformed nanostraws-PC. GFP expression after 48 hours showed a similar trend, but the percentage

of GFP-expressing cells was lower than the YOYO-1-positive cells for all substrates. This result was similar to the findings in Paper I and was now further investigated.

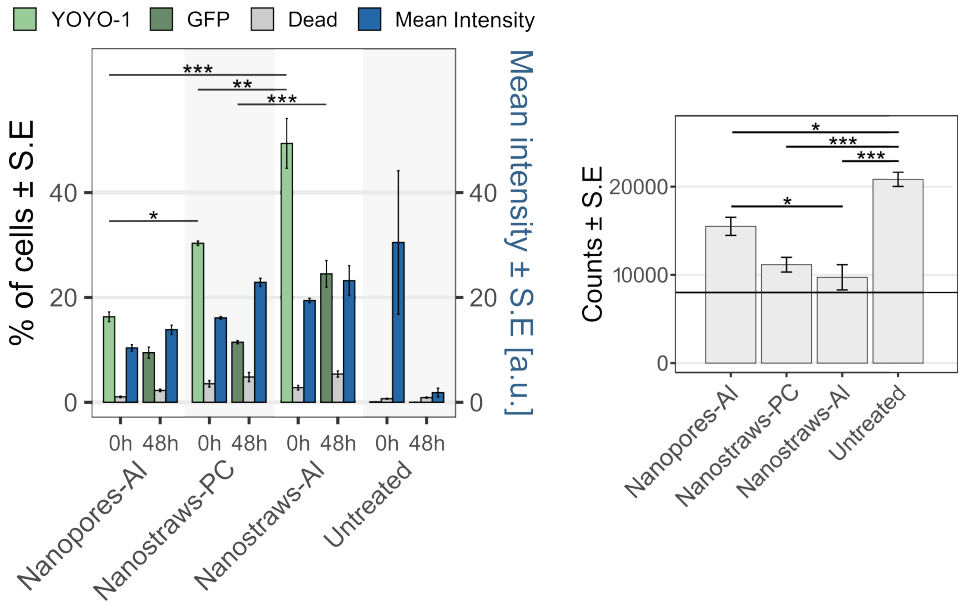

(a) Transfection results

(b) Cell count after 48 hours

Figure 4.9: Comparison of three types of substrates with different surface chemistries and topographies. **(a)** Transfection efficiency immediately after injection (light green), GFP-expression after 48 hours (dark green), as well as cell death (grey) and mean fluorescence intensity (blue) at the two time points. Note that the high mean fluorescence of the control at 0 h is due to the fact that the mean intensity is calculated from positive cells only. As the control has very few positive cells, the mean intensity is, in this case, calculated from outliers. **(b)** Cell count 48 hours after transfection and seeding of 8000 cells per sample, indicated by the black horizontal line. (n=3, statistics: ANOVA and Tukey Post Hoc test with ***: p<0.001, **: p<0.01, *:p<0.05.)

As previously stated, the discrepancy in percentage between GFP-expressing cells and immediately transfected cells could arise from lower proliferation or cell death, suggested by the difference in cell count 48 hours after transfection (Figure 4.5 and 4.9a). When lower proliferation was ruled out, cell death was instead indicated to be the cause. However, the cell death assessed using flow cytomtry was low at both time points (Figure 4.9a). Another possible explanation for the lower cell count was that cells detached from the substrate and thereby were not included in the flow cytometry analysis. After acquiring time-lapse images of cells transfected with the various substrates using phase holographic microscopy, we could conclude that this was indeed the case. For nanostraws-Al, a small fraction of cells adhered properly and divided (forming small clusters), while most were not and detached from the substrate. Additional fluorescence images showed that GFP-expressing cells were rarely a part of the clusters of normally adhering and dividing cells. Control experiments without plasmids indicated that the plasmids were the cause of the cell detachment. With the highest transfection efficiency correlating with the lowest cell count (nanostraws-Al in

Figure 4.9), there was possibly a dose-dependence as well, with more plasmids being more cytotoxic. This showed that maximising cargo delivery may not always be the most suitable goal. Instead, the amount of delivered plasmids should be adjusted to achieve the desired effect while maintaining cell viability, in which cell count is an essential factor to consider.

Chapter 5

Results - Modification of gene expression using nanoelectroporation

The third paper revolves around applying the nanoelectroporation method towards an application within diabetes research, i.e. altering insulin gene expression in clonal β-cells. This was achieved using the CRISPRi system (described in section 2.4), with a repressor called Super Krüppel-associated Box Domain (SKD) bound to the CRISPR-dCas9 [104]. This system represents a first step toward epigenetic editing, for which the CRISPRi system can be used to develop a protocol and act as a proof of principle.

5.1 Downregulation of *Ins1* gene expression - Results of Paper III

The CRISPRi complex was transfected in two parts: one plasmid coding for the sgRNA (3.5 kbps) and one for the dCas9-SKD (8 kbps). Based on the results of papers I and II, alumina-coated nanopores were chosen for this project. Before transfecting the CRISPRi system, some optimisation was first carried out to adapt the method to the dCas9-SKD plasmid, which was considerably larger than the cargo molecules we used in Papers I and II.

First, the optimal nanopore diameter and voltage for the dCas9-SKD plasmid alone were investigated (see Figure 5.1), because it was the largest plasmid used in the CRISPRi system and hence the most difficult to transfect. Moreover, the transfection efficiency for a plasmid in the same size range as the sgRNA plasmid was established already in paper II (Al-surface chemistry in Figure 4.7c).

Figure 5.1 clearly shows that a larger pore diameter led to higher cell death for both 22 V and

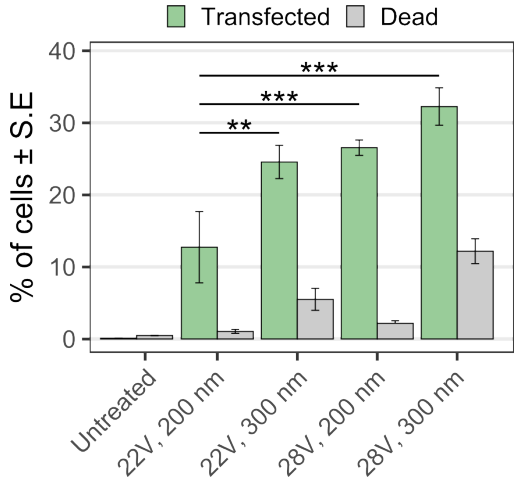

Figure 5.1: Optimisation of nanopore size and voltage for the dCas9-SKD plasmid stained with YOYO-1. The same DNA concentration as in Papers I and II was employed (200 ng/µl). The percentage of transfected cells and dead cells immediately after transfection is shown in green and grey, respectively. (n=3, statistics: ANOVA and Tukey Post Hoc test with ***: p<0.001 and **: p<0.01)

28 V. Therefore, a pore diameter of 200 nm was chosen for further experiments. Regarding voltage, 28 V was the better choice, since it only had a slightly lower cell viability compared to when applying 22 V, while the transfection efficiency was significantly higher. Hence, for the remaining experiments, we used a 200 nm pore diameter and applied 28 V across the nanopore substrate.

Next, we tested the transfection efficiency when two plasmids of different sizes, similar to the CRISPRi system were transfected simultaneously and whether the transfected cells processed the plasmids during the 48 hours between transfection and analysis (same period as for the upcoming experiments on gene expression modification). To assess this, the dCas9-SKD plasmid was transfected together with the pMAX plasmid used in previous papers. The pMAX plasmid had the same size as the sgRNA plasmid, with the advantage that it encodes a GFP with more reliable expression. It therefore mimicked the sgRNA plasmid, but with a strong fluorescence reporter, which made analysis easier. The resulting GFP-expression, assessed 48 hours after transfection, can be seen in Figure 5.2. Approximately 24% of the cells showed a GFP signal. This meant that 24% of the cells were transfected with and processed the pMAX plasmid when transfected together with the dCas9-SKD plasmid. However, since the dCas9-SKD plasmid did not have a reporter, this result did not say anything about the transfection efficiency of that plasmid. Yet, the results shown in Figures 5.1 and 5.2 gave an indication of the transfection efficiency to expect for the CRISPRi system (around 25% of transfected cells).

Lastly, the rat clonal β-cells were injected with the CRISPRi system to achieve downreg-

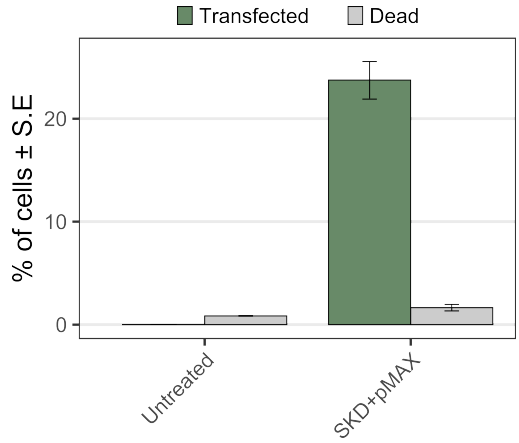

Figure 5.2: GFP expression (green) and cell death (grey) 48 hours after transfection with dCas9-SKD and pMAX plasmids. The GFP reporter is located on the pMAX plasmid.

ulation of the *Ins1* gene expression, evaluated using qPCR. Two types of control samples were used to assess the downregulation: untreated cells and cells transfected with a dCas9 with a No Effector Domain (NED) instead of SKD. The dCas9-NED was almost identical to dCas9-SKD except that it did not contain a transcription factor and should, therefore, not affect the expression of *Ins1*. These two controls, together with the reference gene *Hprt1* (a gene coding for an enzyme that recycles building blocks for DNA and RNA, that is assumed to be stably expressed across different samples), were then used to determine the relative gene expression of *Ins1* between samples and controls as described in section 3.4.5. The result can be seen in Figure 5.3. In Figure 5.3a, the mean relative expression of all experiments (n=19) is displayed, while in Figure 5.3b, the pairs of control (dCas9-NED) and sample (dCas9-SKD) for each experiment are indicated.

There was a significant downregulation of the *Ins1* gene expression for cells transfected with SKD compared to NED. This result demonstrated that the CRISPRi system worked - the sgRNA guided dCas9 to the correct location, and SKD had its intended effect in the *Ins1* gene expression. The difference in mean relative expression was, however, not very large. That was most likely due to a majority of the cells not being successfully transfected, as indicated in Figures 5.1 and 5.2. Sorting cells that are successfully transfected, using fluorescence-activated cell sorting (FACS), could possibly improve the results. In addition, the *Ins1* gene is highly expressed in this cell type and even after downregulation, there could be many mRNA copies left in the cell. Despite these challenges, Figure 5.3b shows that downregulation was achieved in 15 out of 19 experiments. These results shows that the CRISPRi system can be used to downregulate gene expression, which opens up for using it to test the effect of different epigenetic modifications on cell function in the future.

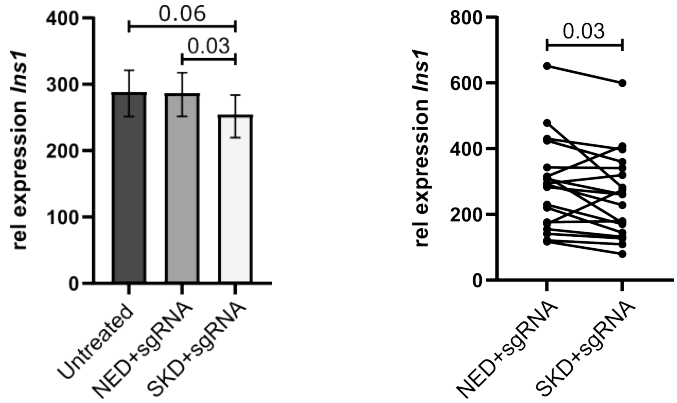

(a) Mean relative expression **(b)** Pairs for each experiment

Figure 5.3: Relative gene expression of clonal β-cells transfected with plasmids coding for dCas9-NED and sgRNA (NED+sgRNA), or dCas9-SKD and sgRNA (SKD+sgRNA). **(a)** Mean relative gene expression of all experiments (n=19). **(b)** Paired results for NED and SKD from each experiment. The indicated p-values of 0.03 and 0.06 were calculated with a Wilcoxon test.

Chapter 6

Conclusion and outlook

In this doctoral thesis, I have explored the use of nanoelectroporation as a transfection method towards an application within diabetes research. More specifically, the potential to use nanoelectroporation to epigenetically modify gene expression of clonal β-cells could open for studying specific molecular changes related to type 2 diabetes and for using it in therapeutic applications. Nanoelectroporation offers a gentle and efficient approach for delivering molecules directly to the cytosol of cells, circumventing the endolysosomal pathway. Although nanoelectroporation has been used on several cell types with various applications in mind, so far, no one has targeted β-cells. That gap is what I aimed to fill during my five years of research. My work can be summarised into three main parts: the optimisation of the nanoelectroporation method parameters, the investigation of how the method affects the long-term viability and cell count, and a proof of principle for regulating insulin gene expression.

Since nanoelectroporation had not been used on rat clonal β-cells before, many parameters needed to be optimised. Some of the parameters we optimised focused on the adaptation of the method for use on rat clonal β-cells, such as voltage and cell density. The results showed that selecting the optimal voltage requires finding the balance between transfection efficiency and cell viability. Moreover, cell density should be chosen such that all cells are in contact with the substrate while as many cells as possible are available for subsequent analysis. Investigating the effect of the cargo buffer conductivity provided us with a better general understanding of the method. Previously, the cargo buffer conductivity had been chosen arbitrarily; however, in my thesis, we found it to have a significant effect on the transfection efficiency of plasmids due to the large differences in voltage drop across the substrate for different conductivities, affecting electrophoresis. The highest voltage drop was achieved using MQ water, which was subsequently used as the cargo solution. Concerning parameters related to the substrate, we demonstrated that the porosity needed to be

high enough for cells to interface with a sufficient number of nanopores/nanostraws, that a larger pore diameter led to higher cell death, and that surface chemistry had a dramatic impact on transfection. The addition of an alumina coating on the substrates considerably increased the transfection efficiency compared to PC or PVP surfaces. Time lapse images of cells on the different substrates showed superior cell adherence on alumina substrates, suggesting that the better transfection efficiency on these substrates is due to a tighter seal between cells and substrate.

Comparing nanopores and nanostraws showed that, while nanostraws delivered more plasmids per cell, the fraction of cells expressing the plasmid after 48 hours was lower than for nanopores. This comparison raised the issue of long-term viability. Our results showed that transfection did not always result in an equal number of cells expressing the plasmid as the number of cells immediately transfected. Additionally, 48 hours after delivery, all transfected samples had a significantly lower cell count than untreated cells, with nanostraws resulting in a lower cell count compared to nanopores. We found that the lower cell count was caused by cytotoxicity from excessive delivery of plasmids. A combination of time-lapse images and fluorescent images showed that many of the transfected cells detached and were not included in the final analysis due to washing steps. Lastly, control experiments without plasmids showed that the nanoelectroporation method in itself did not cause any cell detachment. The fact that nanostraws delivered more plasmids to the cells than nanopores, and resulted in a higher number of detached cells, suggested that our initial aim, to maximise plasmid delivery, may not always be the appropriate objective.

In the last study, we investigated whether we could downregulate insulin expression by injecting the CRISPRi system in clonal β-cells using nanoelectroporation. The CRISPRi system consisted of an sgRNA, a dCas9, and an artificial transcription factor that inhibited gene expression (repressor). This system was injected in the form of two plasmids, with one plasmid coding for the sgRNA and one for the dCas9 and repressor. The plasmids in this project were larger than those we previously used. After some optimisation, we found that the estimated transfection efficiency was roughly 25%. When injecting CRISPRi, we achieved a decrease in relative expression of *Ins1* in a majority of the experiments (15 out of 19), confirming that the CRISPRi system worked. This resulted in a significant downregulation of *Ins1* gene expression compared to cells injected with the same plasmids without the repressor. The difference in mean relative expression was relatively small; however, considering the estimated 25% transfection efficiency, the achieved downregulation is quite striking. Indeed, the *Ins1* gene is highly expressed in this cell type, and although possibly 75% of the cells have normal expression levels, the downregulation is significant. With these results, we showed that nanoelectroporation can deliver the CRIPRi system in the form of large plasmids to affect gene expression, which could be further developed to be used for epigenetic editing.

Looking forward, to further improve our nanoelectroporation setup, I believe the homo-

geneity and fine-tuning of delivery need to be addressed. The amount of delivered cargo, although probably most critical for plasmids, should be possible to adjust while still transfecting the same number of cells. Changing the top electrode geometry, from a wire to a stub, might help make the transfection more homogeneous [81]. Also, the random distribution of pores in the track-etched PC membranes might cause cells to interface with different numbers of nanopores/nanostraws, contributing to the varying amount of delivered cargo. Instead, using a substrate with regularly spaced nanopores or nanostraws would allow the pitch to be tuned to increase the homogeneity.

Although downregulation of gene expression using an artificial transcription factor is a result in itself, the end goal is to replace it with an epigenetic modifier, such as an DMTE (which methylates DNA). By doing so, the effect of epigenetic changes related to type 2 diabetes can be further explored, and the cause-and-effect relationship between the disease and epigenetic modifications better determined. By using nanoelectroporation, the negative safety aspects associated with viral transduction would also be circumvented, thereby opening the possibility for therapeutic applications of epigenetics in type 2 diabetes. Moreover, nanoelectroporation is not limited to β-cells and could also be used for epigenetic modification in other cell types and diseases.

References

[1] Antonio Ceriello and Stephen Colagiuri. IDF global clinical practice recommendations for managing type 2 diabetes–2025. *Diabetes Research and Clinical Practice*, page 112152, 2025.

[2] Ken Suzuki, Konstantinos Hatzikotoulas, Lorraine Southam, Henry J Taylor, Xianyong Yin, Kim M Lorenz, Ravi Mandla, Alicia Huerta-Chagoya, Giorgio EM Melloni, Stavroula Kanoni, et al. Genetic drivers of heterogeneity in type 2 diabetes pathophysiology. *Nature*, 627(8003):347–357, 2024.

[3] Michel Lopes Leite, Kamila Botelho Sampaio de Oliveira, Victor Albuquerque Cunha, Simoni Campos Dias, Nicolau Brito da Cunha, and Fabricio F Costa. Epigenetic therapies in the precision medicine era. *Advanced Therapeutics*, 3(8):1900184, 2020.

[4] Tina Rönn, Jones K Ofori, Alexander Perfilyev, Alexander Hamilton, Karolina Pircs, Fabian Eichelmann, Sonia Garcia-Calzon, Alexandros Karagiannopoulos, Hans Stenlund, Anna Wendt, et al. Genes with epigenetic alterations in human pancreatic islets impact mitochondrial function, insulin secretion, and type 2 diabetes. *Nature Communications*, 14(1):8040, 2023.

[5] Weibo Yu, Shivani Sharma, Elizabeth Rao, Amy C Rowat, James K Gimzewski, Dong Han, and Jianyu Rao. Cancer cell mechanobiology: a new frontier for cancer research. *Journal of the National Cancer Center*, 2(1):10–17, 2022.

[6] Dario F De Jesus and Rohit N Kulkarni. Epigenetic modifiers of islet function and mass. *Trends in Endocrinology & Metabolism*, 25(12):628–636, 2014.

[7] Martin Jinek, Krzysztof Chylinski, Ines Fonfara, Michael Hauer, Jennifer A Doudna, and Emmanuelle Charpentier. A programmable dual-RNA–guided DNA endonuclease in adaptive bacterial immunity. *science*, 337(6096):816–821, 2012.

[8] Nobel Prize in Chemistry 2020. `https://www.nobelprize.org/prizes/chemistry/2020/summary/`. Accessed: 2025-07-09.

[9] Tianxiang Li, Yanyan Yang, Hongzhao Qi, Weigang Cui, Lin Zhang, Xiuxiu Fu, Xiangqin He, Meixin Liu, Pei-feng Li, and Tao Yu. CRISPR/Cas9 therapeutics: progress and prospects. *Signal transduction and targeted therapy*, 8(1):36, 2023.

[10] Charlotte Ling, Karl Bacos, and Tina Rönn. Epigenetics of type 2 diabetes mellitus and weight change—a tool for precision medicine? *Nature Reviews Endocrinology*, 18(7):433–448, 2022.

[11] Hsui Bin Sun, Jin Shen, and Hiroki Yokota. Size-dependent positioning of human chromosomes in interphase nuclei. *Biophysical journal*, 79(1):184–190, 2000.

[12] Charlotte Ling and Tina Rönn. Epigenetics in human obesity and type 2 diabetes. *Cell metabolism*, 29(5):1028–1044, 2019.

[13] José M Ordovás and Caren E Smith. Epigenetics and cardiovascular disease. *Nature Reviews Cardiology*, 7(9):510–519, 2010.

[14] Shannon Byler, Sarah Goldgar, Sarah Heerboth, Meghan Leary, Genevieve Housman, Kimberly Moulton, and Sibaji Sarkar. Genetic and epigenetic aspects of breast cancer progression and therapy. *Anticancer research*, 34(3):1071–1077, 2014.

[15] Gaochen Jin and Bomyi Lim. Epigenome editing and epigenetic gene regulation in disease phenotypes. *Korean Journal of Chemical Engineering*, 39(6):1361–1367, 2022.

[16] Sarah Heerboth, Karolina Lapinska, Nicole Snyder, Meghan Leary, Sarah Rollinson, and Sibaji Sarkar. Use of epigenetic drugs in disease: an overview. *Genetics & epigenetics*, 6:GEG–S12270, 2014.

[17] Joshua Lederberg. Cell genetics and hereditary symbiosis. *Physiological reviews*, 32(4):403–430, 1952.

[18] Bradford Talcott and Mary Shannon Moore. Getting across the nuclear pore complex. *Trends in cell biology*, 9(8):312–318, 1999.

[19] Tokuko Haraguchi, Takako Koujin, Tomoko Shindo, Şükriye Bilir, Hiroko Osakada, Kohei Nishimura, Yasuhiro Hirano, Haruhiko Asakawa, Chie Mori, Shouhei Kobayashi, et al. Transfected plasmid DNA is incorporated into the nucleus via nuclear envelope reformation at telophase. *Communications Biology*, 5(1):78, 2022.

[20] Delphine Lechardeur and Gergely L Lukacs. Nucleocytoplasmic transport of plasmid DNA: a perilous journey from the cytoplasm to the nucleus. *Human gene therapy*, 17(9):882–889, 2006.

[21] Yi Lin, Ernst Wagner, and Ulrich Lächelt. Non-viral delivery of the CRISPR/Cas system: DNA versus RNA versus RNP. *Biomaterials Science*, 10(5):1166–1192, 2022.

[22] Jie Li, Joachim Justad Røise, Maomao He, Riddha Das, and Niren Murthy. Non-viral strategies for delivering genome editing enzymes. *Advanced Drug Delivery Reviews*, 168:99–117, 2021.

[23] Philip L Felgner, Thomas R Gadek, Marilyn Holm, Richard Roman, Hardy W Chan, Michael Wenz, Jeffrey P Northrop, Gordon M Ringold, and Mark Danielsen. Lipofection: a highly efficient, lipid-mediated DNA-transfection procedure. *Proceedings of the National Academy of Sciences*, 84(21):7413–7417, 1987.

[24] C Anamourlis. The cell membrane. *Southern African Journal of Anaesthesia and Analgesia*, 26(6):S1–7, 2020.

[25] Ira Mellman. Endocytosis and molecular sorting. *Annual review of cell and developmental biology*, 12(1):575–625, 1996.

[26] Alexander Pfeifer and Inder M Verma. Gene therapy: promises and problems. *Annual review of genomics and human genetics*, 2(1):177–211, 2001.

[27] Tae Kyung Kim and James H Eberwine. Mammalian cell transfection: the present and the future. *Analytical and bioanalytical chemistry*, 397:3173–3178, 2010.

[28] Niels-Bjarne Woods, Arne Muessig, Manfred Schmidt, Johan Flygare, Karin Olsson, Patrick Salmon, Didier Trono, Christof Von Kalle, and Stefan Karlsson. Lentiviral vector transduction of NOD/SCID repopulating cells results in multiple vector integrations per transduced cell: risk of insertional mutagenesis. *Blood, The Journal of the American Society of Hematology*, 101(4):1284–1289, 2003.

[29] Elaine T Schenborn. Transfection technologies. *Transcription factor protocols*, pages 91–102, 2000.

[30] Agnieszka Fus-Kujawa, Pawel Prus, Karolina Bajdak-Rusinek, Paulina Teper, Katarzyna Gawron, Agnieszka Kowalczuk, and Aleksander L Sieron. An overview of methods and tools for transfection of eukaryotic cells in vitro. *Frontiers in bioengineering and biotechnology*, 9:701031, 2021.

[31] Kaitlin Mrksich, Marshall S Padilla, and Michael J Mitchell. Breaking the final barrier: Evolution of cationic and ionizable lipid structure in lipid nanoparticles to escape the endosome. *Advanced drug delivery reviews*, 214:115446, 2024.

[32] Dehua Pei and Marina Buyanova. Overcoming endosomal entrapment in drug delivery. *Bioconjugate chemistry*, 30(2):273–283, 2018.

[33] Ruvanthi N Kularatne, Rachael M Crist, and Stephan T Stern. The future of tissue-targeted lipid nanoparticle-mediated nucleic acid delivery. *Pharmaceuticals*, 15(7):897, 2022.

[34] Sushmita Chatterjee, Edo Kon, Preeti Sharma, and Dan Peer. Endosomal escape: A bottleneck for LNP-mediated therapeutics. *Proceedings of the National Academy of Sciences*, 121(11):e2307800120, 2024.

[35] Kate Rhodes, Imran Clark, Michelle Zatcoff, Trisha Eustaquio, Kwame L Hoyte, and Manfred R Koller. Cellular laserfection. *Methods in cell biology*, 82:309–333, 2007.

[36] Joseph Rich, Zhenhua Tian, and Tony Jun Huang. Sonoporation: Past, present, and future. *Advanced materials technologies*, 7(1):2100885, 2022.

[37] Apresio K Fajrial, Qing Qing He, Nurul I Wirusanti, Jill E Slansky, and Xiaoyun Ding. A review of emerging physical transfection methods for CRISPR/Cas9-mediated gene editing. *Theranostics*, 10(12):5532, 2020.

[38] Xiaofan Du, Jing Wang, Quan Zhou, Luwei Zhang, Sijia Wang, Zhenxi Zhang, and Cuiping Yao. Advanced physical techniques for gene delivery based on membrane perforation. *Drug delivery*, 25(1):1516–1525, 2018.

[39] Sophie Mehier-Humbert and Richard H Guy. Physical methods for gene transfer: improving the kinetics of gene delivery into cells. *Advanced drug delivery reviews*, 57(5):733–753, 2005.

[40] Eberhard Neumann, M Schaefer-Ridder, Y Wang, and PhH Hofschneider. Gene transfer into mouse lyoma cells by electroporation in high electric fields. *The EMBO journal*, 1(7):841–845, 1982.

[41] Mayya Tokman, Jane HyoJin Lee, Zachary A Levine, Ming-Chak Ho, Michael E Colvin, and P Thomas Vernier. Electric field-driven water dipoles: nanoscale architecture of electroporation. *PloS one*, 8(4):e61111, 2013.

[42] Angelika Vižintin and Damijan Miklavčič. The electropermeome: cellular response to electroporation. *Slovenian Medical Journal*, 91(11-12):483–495, 2022.

[43] Tadej Kotnik, Wolfgang Frey, Martin Sack, Saša Haberl Meglič, Matjaž Peterka, and Damijan Miklavčič. Electroporation-based applications in biotechnology. *Trends in biotechnology*, 33(8):480–488, 2015.

[44] Martin L Yarmush, Alexander Golberg, Gregor Serša, Tadej Kotnik, and Damijan Miklavčič. Electroporation-based technologies for medicine: principles, applications, and challenges. *Annual review of biomedical engineering*, 16(1):295–320, 2014.

[45] Esther Lestrell, Fernando Patolsky, Nicolas H Voelcker, and Roey Elnathan. Engineered nano-bio interfaces for intracellular delivery and sampling: applications, agency and artefacts. *Materials Today*, 33:87–104, 2020.

[46] Alex K Shalek, Jacob T Robinson, Ethan S Karp, Jin Seok Lee, Dae-Ro Ahn, Myung-Han Yoon, Amy Sutton, Marsela Jorgolli, Rona S Gertner, Taranjit S Gujral, et al. Vertical silicon nanowires as a universal platform for delivering biomolecules into living cells. *Proceedings of the National Academy of Sciences*, 107(5):1870–1875, 2010.

[47] Alex K Shalek, Jellert T Gaublomme, Lili Wang, Nir Yosef, Nicolas Chevrier, Mette S Andersen, Jacob T Robinson, Nathalie Pochet, Donna Neuberg, Rona S Gertner, et al. Nanowire-mediated delivery enables functional interrogation of primary immune cells: application to the analysis of chronic lymphocytic leukemia. *Nano letters*, 12(12):6498–6504, 2012. `https://pubs.acs.org/doi/full/10.1021/nl3042917`.

[48] Mohamed Rahamathulla, Santhosh Murugesan, DV Gowda, Ali H Alamri, Mohammed Muqtader Ahmed, Riyaz Ali M Osmani, Sathish Ramamoorthy, and Balamuralidhara Veeranna. The use of nanoneedles in drug delivery: an overview of recent trends and applications. *AAPS PharmSciTech*, 24(8):216, 2023.

[49] Ciro Chiappini, Enrica De Rosa, JO Martinez, Xuewu Liu, Joe Steele, MM Stevens, and Ennio Tasciotti. Biodegradable silicon nanoneedles delivering nucleic acids intracellularly induce localized in vivo neovascularization. *Nature materials*, 14(5):532–539, 2015.

[50] Ciro Chiappini, Jonathan O Martinez, Enrica De Rosa, Carina S Almeida, Ennio Tasciotti, and Molly M Stevens. Biodegradable nanoneedles for localized delivery of nanoparticles in vivo: exploring the biointerface. *ACS nano*, 9(5):5500–5509, 2015.

[51] Sahana Gopal, Ciro Chiappini, Jelle Penders, Vincent Leonardo, Hyejeong Seong, Stephen Rothery, Yuri Korchev, Andrew Shevchuk, and Molly M Stevens. Porous silicon nanoneedles modulate endocytosis to deliver biological payloads. *Advanced Materials*, 31(12):1806788, 2019.

[52] Niklas Sköld, Waldemar Hällström, Henrik Persson, Lars Montelius, Martin Kanje, Lars Samuelson, Christelle N Prinz, and Jonas O Tegenfeldt. Nanofluidics in hollow nanowires. *Nanotechnology*, 21(15):155301, 2010.

[53] Henrik Persson, Jason P Beech, Lars Samuelson, Stina Oredsson, Christelle N Prinz, and Jonas O Tegenfeldt. Vertical oxide nanotubes connected by subsurface microchannels. *Nano Research*, 5(3):190–198, 2012.

[54] Alexander M Xu, Amin Aalipour, Sergio Leal-Ortiz, Armen H Mekhdjian, Xi Xie, Alexander R Dunn, Craig C Garner, and Nicholas A Melosh. Quantification of nanowire penetration into living cells. *Nature communications*, 5(1):3613, 2014.

[55] Jules J VanDersarl, Alexander M Xu, and Nicholas A Melosh. Nanostraws for direct fluidic intracellular access. *Nano letters*, 12(8):3881–3886, 2012.

[56] Gen He, Ning Hu, Alexander M Xu, Xiangling Li, Yunlong Zhao, and Xi Xie. Nanoneedle platforms: the many ways to pierce the cell membrane. *Advanced functional materials*, 30(21):1909890, 2020.

[57] Ying Wang, Yang Yang, Li Yan, So Ying Kwok, Wei Li, Zhigang Wang, Xiaoyue Zhu, Guangyu Zhu, Wenjun Zhang, Xianfeng Chen, et al. Poking cells for efficient vector-free intracellular delivery. *Nature communications*, 5(1):4466, 2014.

[58] Sunwoong Bae, Seunghye Park, Jung Kim, Jong Seob Choi, Kyung Hoon Kim, Donguk Kwon, EonSeon Jin, Inkyu Park, Do Hyun Kim, and Tae Seok Seo. Exogenous gene integration for microalgal cell transformation using a nanowire-incorporated microdevice. *ACS applied materials & interfaces*, 7(49):27554–27561, 2015.

[59] Gabriele C Messina, Michele Dipalo, Rosanna La Rocca, Pierfrancesco Zilio, Valeria Caprettini, Remo Proietti Zaccaria, Andrea Toma, Francesco Tantussi, Luca Berdondini, and Francesco De Angelis. Spatially, temporally, and quantitatively controlled delivery of broad range of molecules into selected cells through plasmonic nanotubes. *Advanced Materials*, 27(44):7145–7149, 2015.

[60] Manyan Wang, Owe Orwar, Jessica Olofsson, and Stephen G Weber. Single-cell electroporation. *Analytical and bioanalytical chemistry*, 397(8):3235–3248, 2010.

[61] Yuhong Cao, Hui-Jiuan Chen, Ruoyi Qiu, Mina-Elraheb Hanna, Enbo Ma, Martin Hjort, Angela Zhang, Richard S. Lewis, Joseph C. Wu, and Nicholas A. Melosh. Universal intracellular biomolecule delivery with precise dosage control. *Science Advances*, 4(10):eaat8131, 2018.

[62] Elke Hebisch, Martin Hjort, Diogo Volpati, and Christelle N Prinz. Nanostraw-assisted cellular injection of fluorescent nanodiamonds via direct membrane opening. *Small*, 17(7):2006421, 2021.

[63] Juan Jiang, Jing Liu, Xinmin Liu, Xingyuan Xu, Zhengjie Liu, Shuang Huang, Xinshuo Huang, Chuanjie Yao, Xiafeng Wang, Yixin Chen, et al. Coupling of nanostraws with diverse physicochemical perforation strategies for intracellular DNA delivery. *Journal of Nanobiotechnology*, 22(1):131, 2024.

[64] Simon Gravelle. Nanofluidics: a pedagogical introduction. 2016.

[65] Ya Sun, Rui Jiang, Lide Hu, Yongxin Song, and Mengqi Li. Electrokinetic transport phenomena in nanofluidics and their applications. *Electrophoresis*, 44(23):1756–1773, 2023.

[66] Daniel G Haywood, Anumita Saha-Shah, Lane A Baker, and Stephen C Jacobson. Fundamental studies of nanofluidics: nanopores, nanochannels, and nanopipets. *Analytical chemistry*, 87(1):172–187, 2015.

[67] Jules J VanDersarl, Alexander M Xu, and Nicholas A Melosh. Rapid spatial and temporal controlled signal delivery over large cell culture areas. *Lab on a Chip*, 11(18):3057–3063, 2011.

[68] Elad Peer, Arbel Artzy-Schnirman, Lior Gepstein, and Uri Sivan. Hollow nanoneedle array and its utilization for repeated administration of biomolecules to the same cells. *ACS nano*, 6(6):4940–4946, 2012.

[69] Alexander M Xu, Sally A Kim, Derek S Wang, Amin Aalipour, and Nicholas A Melosh. Temporally resolved direct delivery of second messengers into cells using nanostraws. *Lab on a Chip*, 16(13):2434–2439, 2016.

[70] Alexander M Xu, Derek S Wang, Peyton Shieh, Yuhong Cao, and Nicholas A Melosh. Direct intracellular delivery of cell-impermeable probes of protein glycosylation by using nanostraws. *ChemBioChem*, 18(7):623–628, 2017.

[71] Xi Xie, Alexander M Xu, Matthew R Angle, Noureddine Tayebi, Piyush Verma, and Nicholas A Melosh. Mechanical model of vertical nanowire cell penetration. *Nano letters*, 13(12):6002–6008, 2013.

[72] Amin Aalipour, Alexander M Xu, Sergio Leal-Ortiz, Craig C Garner, and Nicholas A Melosh. Plasma membrane and actin cytoskeleton as synergistic barriers to nanowire cell penetration. *Langmuir*, 30(41):12362–12367, 2014.

[73] Xi Xie, Alexander M Xu, Sergio Leal-Ortiz, Yuhong Cao, Craig C Garner, and Nicholas A Melosh. Nanostraw–electroporation system for highly efficient intracellular delivery and transfection. *ACS nano*, 7(5):4351–4358, 2013.

[74] Yuhong Cao, Martin Hjort, Haodong Chen, Fikri Birey, Sergio A Leal-Ortiz, Crystal M Han, Juan G Santiago, Sergiu P Paşca, Joseph C Wu, and Nicholas A Melosh. Nondestructive nanostraw intracellular sampling for longitudinal cell monitoring. *Proceedings of the National Academy of Sciences*, 114(10):E1866–E1874, 2017.

[75] Aihua Zhang, Jiaru Fang, Ji Wang, Xi Xie, Hui-Jiuan Chen, and Gen He. Interrogation on the cellular nano-interface and biosafety of repeated nano-electroporation by nanostraw system. *Biosensors*, 12(7):522, 2022.

[76] Gen He, Jianming Feng, Aihua Zhang, Lingfei Zhou, Rui Wen, Jiangming Wu, Chengduan Yang, Jiang Yang, Chunwei Li, Demeng Chen, et al. Multifunctional branched nanostraw-electroporation platform for intracellular regulation and monitoring of circulating tumor cells. *Nano letters*, 19(10):7201–7209, 2019.

[77] Gyeong Won Lee, Byeongyeon Kim, Tae Wook Lee, Sang-Gu Yim, Ajeesh Chandrasekharan, Hyewon Kim, Sungyoung Choi, and Seung Yun Yang. Nanoporous electroporation needle for localized intracellular delivery in deep tissues. *Bioengineering & Translational Medicine*, 8(4):e10418, 2023.

[78] Rui Wen, Ai-hua Zhang, Di Liu, Jianming Feng, Jiang Yang, Dehua Xia, Ji Wang, Chunwei Li, Tao Zhang, Ning Hu, et al. Intracellular delivery and sensing system based on electroplated conductive nanostraw arrays. *ACS Applied Materials & Interfaces*, 11(47):43936–43948, 2019.

[79] Prithvijit Mukherjee, S Shiva P Nathamgari, John A Kessler, and Horacio D Espinosa. Combined numerical and experimental investigation of localized electroporation-based cell transfection and sampling. *ACS nano*, 12(12):12118–12128, 2018.

[80] Ludwig Schmiderer, Agatheeswaran Subramaniam, Kristijonas Žemaitis, Alexandra Bäckström, David Yudovich, Svetlana Soboleva, Roman Galeev, Christelle N Prinz, Jonas Larsson, and Martin Hjort. Efficient and nontoxic biomolecule delivery to primary human hematopoietic stem cells using nanostraws. *Proceedings of the National Academy of Sciences*, 117(35):21267–21273, 2020.

[81] Cesar A Patino, Nibir Pathak, Prithvijit Mukherjee, So Hyun Park, Gang Bao, and Horacio D Espinosa. Multiplexed high-throughput localized electroporation workflow with deep learning–based analysis for cell engineering. *Science Advances*, 8(29):eabn7637, 2022.

[82] Mara A Pop and Benjamin D Almquist. Controlled delivery of microRNAs into primary cells using nanostraw technology. *Advanced nanobiomed research*, 1(6):2000061, 2021.

[83] Yuhong Cao, Enbo Ma, Stefano Cestellos-Blanco, Bei Zhang, Ruoyi Qiu, Yude Su, Jennifer A Doudna, and Peidong Yang. Nontoxic nanopore electroporation for effective intracellular delivery of biological macromolecules. *Proceedings of the National Academy of Sciences*, 116(16):7899–7904, 2019.

[84] Andy Tay and Nicholas Melosh. Mechanical stimulation after centrifuge-free nanoelectroporative transfection is efficient and maintains long-term T cell functionalities. *Small*, 17(38):2103198, 2021.

[85] Nibir Pathak, Cesar A Patino, Namrata Ramani, Prithvijit Mukherjee, Devleena Samanta, Sasha B Ebrahimi, Chad A Mirkin, and Horacio D Espinosa. Cellular delivery of large functional proteins and protein–nucleic acid constructs via localized electroporation. *Nano letters*, 23(8):3653–3660, 2023.

[86] Wonmo Kang, Juan P Giraldo-Vela, S Shiva P Nathamgari, Tammy McGuire, Rebecca L McNaughton, John A Kessler, and Horacio D Espinosa. Microfluidic device for stem cell differentiation and localized electroporation of postmitotic neurons. *Lab on a Chip*, 14(23):4486–4495, 2014.

[87] Gen He, Hui-Jiuan Chen, Di Liu, Yuping Feng, Chengduan Yang, Tian Hang, Jiangming Wu, Yuhong Cao, and Xi Xie. Fabrication of various structures of nanostraw arrays and their applications in gene delivery. *Advanced Materials Interfaces*, 5(10):1701535, 2018.

[88] Xiangyu Ren, Yi Weng, Ziwei Zhang, Guangjin Pan, Chaobo Li, and Yuhong Cao. Nanopore-based electroporation enables high-efficiency, rapid RNA-mediated reprogramming of primary fibroblasts into human iPSCs. *Nano Letters*, 2025.

[89] Bowen Zhang, Yiming Shi, Daisuke Miyamoto, Koji Nakazawa, and Takeo Miyake. Nanostraw membrane stamping for direct delivery of molecules into adhesive cells. *Scientific reports*, 9(1):6806, 2019.

[90] Arun RK Kumar, Jessalyn Low, Jet Lim, Ba Myint, Xinhong Sun, Ling Wu, Hong Sheng Cheng, Sophronia Yip, Cyrus Zai Ming Cheng, Thamizhanban Manoharan, et al. Non-viral, high throughput genetic engineering of primary immune cells using nanostraw-mediated transfection. *Biomaterials*, 317:123079, 2025.

[91] Andy Tay and Nicholas Melosh. Transfection with nanostructure electro-injection is minimally perturbative. *Advanced therapeutics*, 2(12):1900133, 2019.

[92] Yang Liu, Ludwig Schmiderer, Martin Hjort, Stefan Lang, Tyra Bremborg, Anna Rydström, Axel Schambach, Jonas Larsson, and Stefan Karlsson. Engineered human diamond-blackfan anemia disease model confirms therapeutic effects of clinically applicable lentiviral vector at single-cell resolution. *Haematologica*, 108(11):3095, 2023.

[93] Charis-P Segeritz and Ludovic Vallier. Cell culture: Growing cells as model systems in vitro. In *Basic science methods for clinical researchers*, pages 151–172. Elsevier, 2017.

[94] Véronique Cremers, Riikka L Puurunen, and Jolien Dendooven. Conformality in atomic layer deposition: Current status overview of analysis and modelling. *Applied Physics Reviews*, 6(2), 2019.

[95] Riikka L Puurunen. Surface chemistry of atomic layer deposition: A case study for the trimethylaluminum/water process. *Journal of applied physics*, 97(12), 2005.

[96] Stephen J Pearton and David P Norton. Dry etching of electronic oxides, polymers, and semiconductors. *Plasma Processes and Polymers*, 2(1):16–37, 2005.

[97] Katarzyna Racka-Szmidt, Bartłomiej Stonio, Jarosław Żelazko, Maciej Filipiak, and Mariusz Sochacki. A review: Inductively coupled plasma reactive ion etching of silicon carbide. *Materials*, 15(1):123, 2021.

[98] Bin He, Yang Yang, Muk Fung Yuen, XF Chen, Chun Sing Lee, and WJ Zhang. Vertical nanostructure arrays by plasma etching for applications in biology, energy, and electronics. *Nano Today*, 8(3):265–289, 2013.

[99] Anwar Ul-Hamid. *A beginners' guide to scanning electron microscopy*, volume 1. Springer, 2018.

[100] Inc. AAT Bioquest. Spectrum [YOYO-1]. `https://www.aatbio.com/fluorescence-excitation-emission-spectrum-graph-viewer/yoyo_1`, 2024. Accessed: 2024-10-03.

[101] Binu Kundukad, Jie Yan, and Patrick S Doyle. Effect of YOYO-1 on the mechanical properties of DNA. *Soft matter*, 10(48):9721–9728, 2014.

[102] Aysun Adan, Günel Alizada, Yağmur Kiraz, Yusuf Baran, and Ayten Nalbant. Flow cytometry: basic principles and applications. *Critical reviews in biotechnology*, 37(2):163–176, 2017.

[103] Mercy Lard, Bao D Ho, Jason P Beech, Jonas O Tegenfeldt, and Christelle N Prinz. Use of dielectrophoresis for directing T cells to microwells before nanostraw transfection: modelling and experiments. *RSC advances*, 12(47):30295–30303, 2022.

[104] Rutger AF Gjaltema, Désirée Goubert, Christian Huisman, Consuelo del Pilar García Tobilla, Mihály Koncz, Pytrick G Jellema, Dandan Wu, Uilke Brouwer, Antal Kiss, Pernette J Verschure, et al. KRAB-induced heterochromatin effectively silences PLOD2 gene expression in somatic cells and is resilient to TGFβ1 activation. *International Journal of Molecular Sciences*, 21(10):3634, 2020.

'Mischief Managed!'

Printed by Media-Tryck, Lund 2025 NORDIC SWAN ECOLABEL 3041 0903

LUND UNIVERSITY

Faculty of Engineering
Department of Physics

ISBN 978-91-8104-679-3